JCI The Journal of Clinical Investigation

Sox2 haploinsufficiency primes regeneration and Wnt responsiveness in the mouse cochlea

Patrick J. Atkinson, … , Tomokatsu Udagawa, Alan G. Cheng

J Clin Invest. 2018;128(4):1641-1656. https://doi.org/10.1172/JCI97248.

Research Article **Cell biology** **Neuroscience**

During development, Sox2 is indispensable for cell division and differentiation, yet its roles in regenerating tissues are less clear. Here, we used combinations of transgenic mouse models to reveal that Sox2 haploinsufficiency ($Sox2^{haplo}$) increases rather than impairs cochlear regeneration in vivo. $Sox2^{haplo}$ cochleae had delayed terminal mitosis and ectopic sensory cells, yet normal auditory function. $Sox2^{haplo}$ amplified and expanded domains of damage-induced $Atoh1^{+}$ transitional cell formation in neonatal cochlea. Wnt activation via β-catenin stabilization ($β\text{-catenin}^{GOF}$) alone failed to induce proliferation or transitional cell formation. By contrast, $β\text{-catenin}^{GOF}$ caused proliferation when either $Sox2^{haplo}$ or damage was present, and transitional cell formation when both were present in neonatal, but not mature, cochlea. Mechanistically, $Sox2^{haplo}$ or damaged neonatal cochleae showed lower levels of *Sox2* and *Hes5*, but not of Wnt target genes. Together, our study unveils an interplay between Sox2 and damage in directing tissue regeneration and Wnt responsiveness and thus provides a foundation for potential combinatorial therapies aimed at stimulating mammalian cochlear regeneration to reverse hearing loss in humans.

Sox2 haploinsufficiency primes regeneration and Wnt responsiveness in the mouse cochlea

Patrick J. Atkinson,[1] Yaodong Dong,[1,2] Shuping Gu,[1] Wenwen Liu,[1] Elvis Huarcaya Najarro,[1] Tomokatsu Udagawa,[1] and Alan G. Cheng[1]

[1]Department of Otolaryngology – Head and Neck Surgery, Stanford University School of Medicine, Stanford, California, USA. [2]Department of Otology, Shengjing Hospital of China Medical University, Shenyang, Liaoning, China.

During development, Sox2 is indispensable for cell division and differentiation, yet its roles in regenerating tissues are less clear. Here, we used combinations of transgenic mouse models to reveal that Sox2 haploinsufficiency ($Sox2^{haplo}$) increases rather than impairs cochlear regeneration in vivo. $Sox2^{haplo}$ cochleae had delayed terminal mitosis and ectopic sensory cells, yet normal auditory function. $Sox2^{haplo}$ amplified and expanded domains of damage-induced $Atoh1^+$ transitional cell formation in neonatal cochlea. Wnt activation via β-catenin stabilization ($β\text{-catenin}^{GOF}$) alone failed to induce proliferation or transitional cell formation. By contrast, $β\text{-catenin}^{GOF}$ caused proliferation when either $Sox2^{haplo}$ or damage was present, and transitional cell formation when both were present in neonatal, but not mature, cochlea. Mechanistically, $Sox2^{haplo}$ or damaged neonatal cochleae showed lower levels of *Sox2* and *Hes5*, but not of Wnt target genes. Together, our study unveils an interplay between Sox2 and damage in directing tissue regeneration and Wnt responsiveness and thus provides a foundation for potential combinatorial therapies aimed at stimulating mammalian cochlear regeneration to reverse hearing loss in humans.

Introduction

SRY-box 2 (Sox2) is a SoxB1 HMG domain transcription factor critical for establishing and maintaining the pluripotency of embryonic stem cells (1, 2) and, in combination with other defined factors, induces pluripotent stem cells (3, 4). Sox2 also directs cellular differentiation in multiple developing organs, including the CNS (5–9), retina (10), cochlea (11), hair follicles (12), lens (13), and the foregut and its derivatives (14–17). Besides designating tissue-specific progenitors in these developing organs, Sox2 governs cell specification (10, 11, 17,) with deficiencies leading to anophthalmia and epilepsy as well as trachea-esophageal and genital anomalies in both mice and humans (10, 17–20).

Sox2-expressing somatic stem cells are widely distributed in adult animals and are essential for tissue homeostasis and repair (16, 21–23). For example, Sox2 loss of function impairs adult neurogenesis and tracheal repair (16, 24–26). Moreover, Sox2 is upregulated during spinal cord regeneration, with damage inducing the proliferation of $Sox2^+$ cells, and inhibition of Sox2 limiting their regeneration in a dose-dependent manner (27). Thus, the prevailing notion is that Sox2 insufficiency impairs both the development and regeneration of tissues.

In the developing mouse cochlea, Sox2 expression marks the prosensory region, which harbors cells primed to give rise to the mechanosensory hair cells and nonsensory supporting cells of the organ of Corti. Sox2 is required for hair cell specification, as prosensory cells in Sox2-deficient cochleae fail to acquire a hair cell fate (11, 28). A subset of $Sox2^+$ cells first express the prosensory transcription factor Atoh1 around E13.5 (29). Specified sensory cells expressing Atoh1 then mature by upregulating Pou4f3, a transcription factor linked with inherited progressive hearing loss in humans (30, 31), as well as Gfi1 (32) and myosin 7a (33). Conversely, Sox2 is downregulated in maturing hair cells and becomes undetectable in the early postnatal period, while adjacent supporting cells maintain Sox2 expression (34). By binding to its enhancer region, Sox2 can directly activate Atoh1 (35–38) and is sufficient for inducing ectopic sensory hair cells in vitro (38) and in vivo (39) in the embryonic cochlea. A subsequent reduction of Sox2 expression is also necessary for hair cell maturation, as high levels of Sox2 antagonize Atoh1 and prevent hair cell formation when overexpressed in vitro (28, 35), and Sox2 activates repressors of Atoh1 (40). Because Sox2 is initially required for hair cell specification and subsequently inhibits hair cell differentiation, its relationship with hair cell formation is coined an "incoherent feed-forward loop" (41).

Here, we examined the effects of Sox2 haploinsufficiency on cell division and hair cell regeneration in response to damage in the postnatal cochlea. We found that Sox2-haploinsufficient mice had extranumerary cochlear hair cells and normal auditory function in adulthood. Although terminal mitosis normally occurs around E14.5 (42), supporting cells in the postnatal Sox2-haploinsufficient cochlea still divided. After hair cell ablation in the neonatal cochlea, supporting cells that proliferate and form new hair cells are limited in number and spatially restricted (43). In the damaged Sox2-haploinsufficient cochlea, we found an increase in and expansion of the domain of dividing (EdU^+) and transitional ($Atoh1^+$) supporting cells along the cochlea. Moreover,

Authorship note: PJA and YD contributed equally to this work.
Conflict of interest: The authors have declared that no conflict of interest exists.
Submitted: September 1, 2017; **Accepted:** February 1, 2018.
Reference information: *J Clin Invest*. 2018;128(4):1641–1656.
https://doi.org/10.1172/JCI97248.

Sox2 haploinsufficiency and damage act as permissive signals to β-catenin–induced proliferation and formation of transitional cells (cells undergoing a direct phenotypic conversion from supporting cells to hair cell–like cells) in neonatal, but not mature, cochlea. Together, our results show cooperative roles of Sox2 haploinsufficiency and Wnt signaling in regulating the spatiotemporally restricted regenerative responses — proliferation and transitional cell formation — in the postnatal mouse cochlea.

Results

Sox2 haploinsufficiency leads to ectopic hair cell formation and delayed terminal mitosis. The mammalian cochlea is organized as a checkerboard of hair cells intercalated by Sox2$^+$ supporting cells (34) (Figure 1A). In the P5 cochlea, Sox2 expression was robust in most supporting cell subtypes (Hensen's cells, Deiters' cells, pillar cells, and inner phalangeal cells) and also in cells residing in the greater epithelial ridge (Figure 1A). This pattern was confirmed by Cre reporter expression in *Sox2*$^{CreERT2/+}$ *Rosa26R*$^{TdTomato/+}$ cochleae induced on P1 and by GFP expression in *Sox2*$^{GFP/+}$ cochleae (Figure 1, B and C) (21).

To determine whether hair cell formation and proliferation are affected by Sox2 haploinsufficiency, we first examined cochleae from *Sox2*$^{CreERT2/+}$ mice (Figure 1D). The *Sox2*$^{CreERT2/+}$ mouse was generated as an inserted targeted mutation in the single exon of the Sox2 gene (21), resulting in Sox2 haploinsufficiency (Sox2^{haplo}). We performed quantitative PCR (qPCR) on cochleae from P5 *Sox2*$^{CreERT2/+}$ mice and found a reduction of approximately 27.3% in Sox2 expression relative to WT cochleae (Figure 1E, $P < 0.05$). P5 WT cochleae had the normal complement of myosin 7a$^+$ hair cells (3 rows of outer hair cells and 1 row of inner hair cells) (Figure 1F). In *Sox2*$^{CreERT2/+}$ cochleae, we noted extranumerary myosin 7a$^+$ hair cells juxtaposed to inner hair cells (Figure 1G) along the length of the cochlea. We also observed ectopic hair cells along the cochleae from a second Sox2-knockin mouse line (*Sox2*$^{GFP/+}$) (Supplemental Figure 1, B–E; supplemental material available online with this article; https://doi.org/10.1172/JCI97248DS1) (21). On average, we observed 78.2 ± 38.1 and 65.5 ± 27.0 ectopic hair cells in whole cochleae from *Sox2*$^{CreERT2/+}$ and *Sox2*$^{GFP/+}$ mice, respectively, compared with 3.3 ± 1.5 ectopic hair cells in WT control cochleae (Figure 1H).

The last mitotic event in the developing organ of Corti occurs in the basal turn around E14.5 (42). EdU pulses (P2–P4, Figure 1D) failed to label any hair cells or supporting cells in the WT cochlea, confirming its mitotic quiescence (Figure 1F). With the same EdU regimen (Figure 1D and Supplemental Figure 1A), we observed 10.2 ± 4.8 and 22.8 ± 13.8 EdU-labeled supporting cells in the apical turn of *Sox2*$^{CreERT2/+}$ and *Sox2*$^{GFP/+}$ cochleae, respectively (Figure 1, G and I, Supplemental Figure 1C, and Supplemental Table 1). There were no EdU$^+$ supporting cells in the middle or basal turns (Supplemental Figure 1, D and E). To determine the timing of terminal mitosis in *Sox2*$^{CreERT2/+}$ mice, we delayed the EdU injection schedule by 1 day (P3–P5) and failed to detect any EdU-labeled supporting cells in the organ of Corti ($n = 3$, data not shown). This indicates that terminal mitosis is delayed until around P2 in the *Sox2*$^{CreERT2/+}$ cochlea. We confirmed this finding by immunostaining for the proliferation marker Ki67 in *Sox2*$^{CreERT2/+}$ and *Sox2*$^{GFP/+}$ cochleae (P4–P5) and found no Ki67$^+$ cells in the organ of Corti (Supplemental Figure 1, F–H). We also measured the auditory brainstem response (ABR) and distortion product otoacoustic emissions (DPOAEs) and found no statistical differences in thresholds between *Sox2*$^{CreERT2/+}$ mice and WT mice at 4 weeks of age (Figure 1J and Supplemental Figure 1I). These results demonstrate that Sox2 haploinsufficiency (Sox2^{haplo}) leads to delayed terminal mitosis and ectopic inner hair cell formation without compromising auditory function.

Sox2^{haplo} *enhances mitotic regeneration and transitional cell formation*. Our prior work showed that supporting cells in the apical turn mitotically regenerate hair cells after hair cell ablation in the neonatal cochlea (43). Here, we compared damaged (*Pou4f3*$^{DTR/+}$) (44) cochleae with damaged, Sox2^{haplo} (*Pou4f3*$^{DTR/+}$ *Sox2*$^{CreERT2/+}$) cochleae (Figure 2A and Supplemental Figure 3E). Cochleae from WT animals injected with diphtheria toxin (DT) showed no hair cell loss or EdU-labeled supporting cells (Figure 2, B–D). As expected, DT-induced hair cell loss in *Pou4f3*$^{DTR/+}$ mice resulted in a modest increase in EdU$^+$ hair cells (0.3 ± 0.1 per 160 μm, myosin 7a$^+$) and supporting cells (1.4 ± 0.5 per 160 μm, Sox2$^+$myosin 7a$^-$) in the apical turn (Figure 2E and Supplemental Table 1). We found no proliferative cells in the middle or basal turns of the damaged cochlea (Figure 2, F and G). In the *Pou4f3*$^{DTR/+}$ *Sox2*$^{CreERT2/+}$ (damaged, Sox2^{haplo}) cochlea, we found a significantly larger number of EdU-labeled supporting cells (10.3 ± 1.9 per 160 μm) and hair cells (1.5 ± 0.3 per 160 μm) in the apical turn (Figure 2H), with EdU-labeled supporting cells also present in the middle turn (Figure 2I) but not the basal turn (Figure 2J). On average, there was a 9.2-fold increase in the total number of EdU-labeled cells in damaged, Sox2^{haplo} cochleae compared with total numbers in the damaged-only cochleae (Figure 2K and Supplemental Table 1). These results indicate that Sox2^{haplo} increases the degree and expands the domain of damage-induced proliferation along the length of the cochlea.

Hair cell regeneration in the neonatal mammalian cochlea can also occur without an antecedent mitotic event (43, 45), through the direct transition of supporting cells into hair cells. We directly assessed the degree of new hair cell formation through immunostaining of damaged cochleae for the transcription factor Atoh1 (Figure 3, A and B, and Supplemental Figure 3A), which is upregulated in nonmitotic hair cell precursors in the regenerating mouse vestibular system (46, 47). Atoh1 is highly expressed in nascent hair cells in the embryonic cochlea and is rapidly downregulated postnatally (48, 49). In agreement with previous reports, we detected Atoh1 protein expression in hair cells in the E18.5 cochlea and its reduction in a base-to-apex direction between P0 and P3, with no expression detected in hair cells at P4 or in supporting cells at any of these ages (Figure 3C and Supplemental Figure 2, A–L). We examined the P1 *Atoh1*$^{GFP/+}$ cochlea (50) and found a similar apical-basal gradient of GFP expression in hair cells and none in supporting cells (Supplemental Figure 2, M–O). Two days after DT-induced hair cell loss on P1, we detected Atoh1, Sox2 double-positive supporting cells in the apical and middle turns in damaged-only (*Pou4f3*$^{DTR/+}$) mouse cochleae (Figure 3, D and E, and Supplemental Figure 3, B–D). To ascertain whether the Atoh1$^+$ cells were supporting cells acquiring a hair cell phenotype, we examined P3 cochlea and found that Atoh1$^+$Sox2$^+$ supporting cells also expressed Gfi1, another hair cell transcription factor normally absent in supporting cells (Figure 3D and Supplemental Figure 3, F and I). The following day (P4), we found that many Atoh1$^+$Sox2$^+$ cells also expressed myosin 7a in the apical and middle turns and

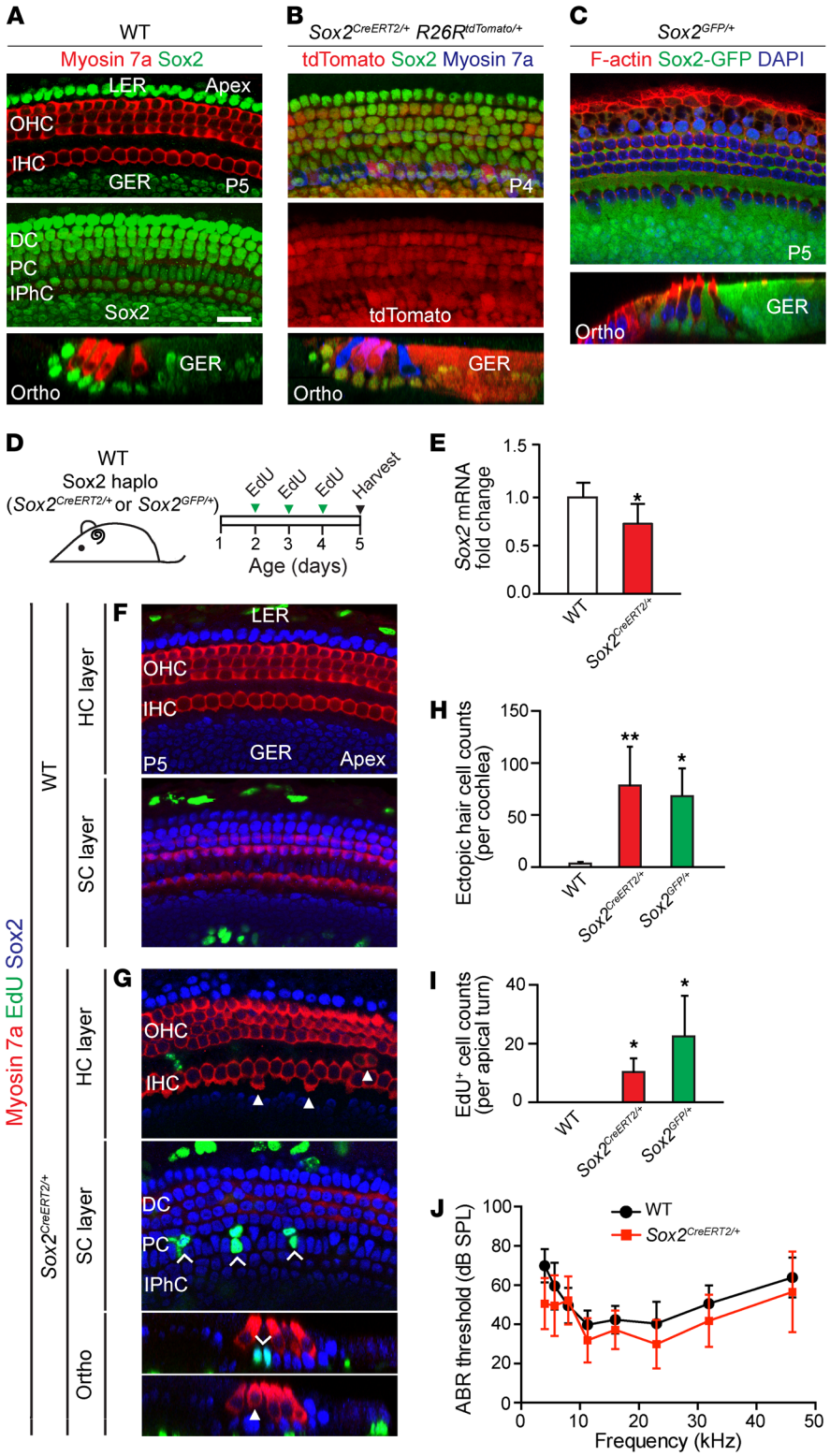

Figure 1. Sox2 haploinsufficiency results in continued proliferation and formation of supernumerary hair cells in the neonatal cochlea. (**A**) Immunostaining of P5 WT cochlea shows Sox2 expression in Hensen's cells, Deiters' cells, pillar cells, and the lateral portion of the greater epithelial ridge. (**B**) Whole-mount preparation of cochlea from P4 *Sox2*$^{CreERT2/+}$ *R26R*$^{tdTomato/+}$ mice given tamoxifen on P2, showing tdTomato expression in supporting cells and some hair cells. (**C**) GFP$^+$ supporting cells in the P5 *Sox2*$^{GFP/+}$ cochlea. (**D**) Schematic of EdU administration to *Sox2*$^{CreERT2/+}$ mice, *Sox2*$^{GFP/+}$ mice, and WT littermates (once daily, P2–P4). haplo, haploinsufficient. (**E**) qPCR showed a significant reduction of *Sox2* expression in *Sox2*$^{CreERT2/+}$ cochleae compared with expression in WT littermates. (**F**) Confocal images show no EdU$^+$ hair cells or supporting cells in the P5 WT cochlea. EdU labeling was seen in cells in the lesser epithelial ridge and greater epithelial ridge. (**G**) *Sox2*$^{CreERT2/+}$ cochlea contained occasional extranumerary hair cells adjacent to inner hair cells (arrowheads). Extranumerary hair cells were noted in all cochlear turns of *Sox2*$^{CreERT2/+}$ mice. Image shows EdU$^+$ supporting cells (chevrons) in the apical turn. No EdU$^+$ hair cells were noted. (**H**) Quantification of extranumerary hair cells in WT, *Sox2*$^{CreERT2/+}$, and *Sox2*$^{GFP/+}$ cochleae. (**I**) Quantification of EdU$^+$ cells in WT, *Sox2*$^{CreERT2/+}$, and *Sox2*$^{GFP/+}$ cochleae. (**J**) P28 *Sox2*$^{CreERT2/+}$ mice had normal ABR thresholds, comparable to those of their WT littermates. DC, Deiters' cell; GER, greater epithelial ridge; HC, hair cell; IHC, inner hair cell; IP, inner pillar cell; IPhC, inner phalangeal cell; LER, lesser epithelial ridge; OHC, outer hair cell; OP, outer pillar cell; Ortho, orthogonal view; PC, pillar cell; SC, supporting cell. Data represent the mean ± SD. $^*P < 0.05$ and $^{**}P < 0.01$, by 2-tailed Student's *t* test. $n = 3–8$. Scale bar: 20 μm.

rarely in the base (9.7 ± 0.6, 5.0 ± 1.0, and 0.3 ± 0.6, respectively) (Figure 3G, Supplemental Figure 3, G and J, and Supplemental Table 2). By P4, when cochlear hair cells normally lack Sox2 expression (Figure 3F), we found that Atoh1$^+$myosin 7a$^+$ cells also expressed Sox2 and Gfi1 (Figure 3G), suggesting that they were supporting cells transitioning into nascent hair cells (Figure 3B). Given these findings, we hereafter define Atoh1$^+$Sox2$^+$ cells as transitional cells. Thus, unlike the proliferative cells that were limited to the apical turn of the damaged cochlea, Atoh1$^+$ transitional cells were found in all 3 cochlear turns (Figure 3I, and Supplemental Figure 3, G and J). In comparison with the damaged-only cochlea (P4), the damaged, Sox2^{haplo} cochlea contained a significantly larger number of transitional cells in all turns (Figure 3, H and I, and Supplemental Figure 3, H and K). Collectively, these

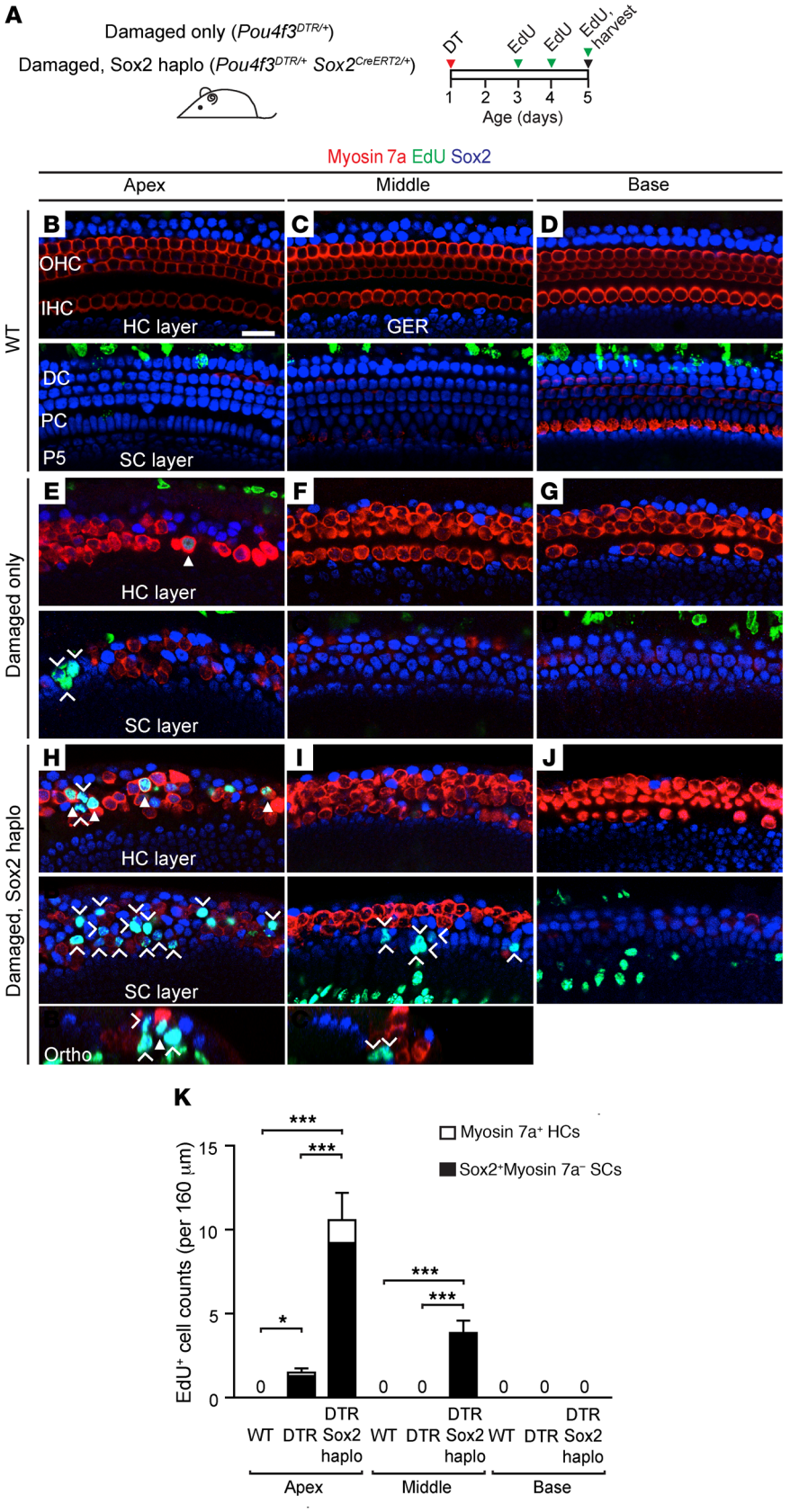

Figure 2. Reduced Sox2 levels enhance and expand the domain of proliferation in the damaged neonatal mouse cochlea. (**A**) Schematic of hair cell ablation in neonatal cochlea. Briefly, *Pou4f3*$^{DTR/+}$ and *Pou4f3*$^{DTR/+}$ *Sox2*$^{CreERT2/+}$ mice were injected with DT on P1 to induce hair cell loss, followed by administration of EdU (P3–P5), and cochleae were examined on P5. (**B**–**D**) No EdU$^+$ hair cells or supporting cells were found in any of the 3 WT cochlear turns. (**E**–**G**) In the *Pou4f3*$^{DTR/+}$ cochlea, after DT-induced hair cell damage, EdU$^+$myosin 7a$^+$ hair cells (arrowhead) and some EdU$^+$Sox2$^+$ supporting cells (chevrons) were observed in the apical turn, but not in the basal or middle turns. (**H**–**J**) In *Pou4f3*$^{DTR/+}$ *Sox2*$^{CreERT2/+}$ cochlea, there was robust EdU labeling of both myosin 7a$^+$ hair cells (arrowheads) and Sox2$^+$ supporting cells (chevrons) in the apical turn. EdU$^+$Sox2$^+$ supporting cells were also found in the middle turn. (**K**) Quantification of EdU$^+$myosin 7a$^+$ hair cells and myosin 7a$^-$Sox2$^+$ supporting cells per cochlear turn. Data represent the mean ± SD. $^*P < 0.05$ and $^{***}P < 0.001$, by 1-way ANOVA with Holm-Sidak multiple comparisons test. n = 5–6. Scale bar: 20 μm.

results suggest that Sox2^{haplo} enhances transitional cell formation in the damaged neonatal cochlea.

Sox2^{haplo} promotes the survival of regenerated hair cells. A previous study showed that regenerated hair cells in the neonatal mouse cochlea undergo subsequent cell death (51). To determine whether Sox2^{haplo} promotes the survival of regenerated hair cells, we compared the damaged, Sox2^{haplo} cochlea with the damaged-only cochlea on P21 (after treatment with DT on P1 and with EdU from P3 to P5) (Supplemental Figure 4A). As expected, we detected no EdU incorporation in the WT cochlea (Supplemental Figure 4B). We found that the damaged-only cochlea contained few hair cells among disorganized supporting cells in the apical turn, with occasional EdU labeling of each cell type (Supplemental Figure 4, C and F). In contrast, the Sox2^{haplo}, damaged cochleae had significantly more EdU$^+$ hair cells and supporting cells in the apical turn than did the damaged-only cochleae (Supplemental Figure 4, D and F). Early after damage (P5, P7, and P10), we found a significantly greater number of hair cells in most turns of the Sox2^{haplo}, damaged cochleae than in the damaged-only cochleae, even though there were few EdU-labeled cells in the middle turn and none in the basal turn on P5 (Supplemental Tables 1 and 3). By P21, both the damaged-only and Sox2^{haplo}, damaged cochleae had a gradual loss of hair cells and EdU-labeled cells (Supplemental Figure 4, E and F, and Supplemental Table 3), with hair cells remaining only in the apical turn.

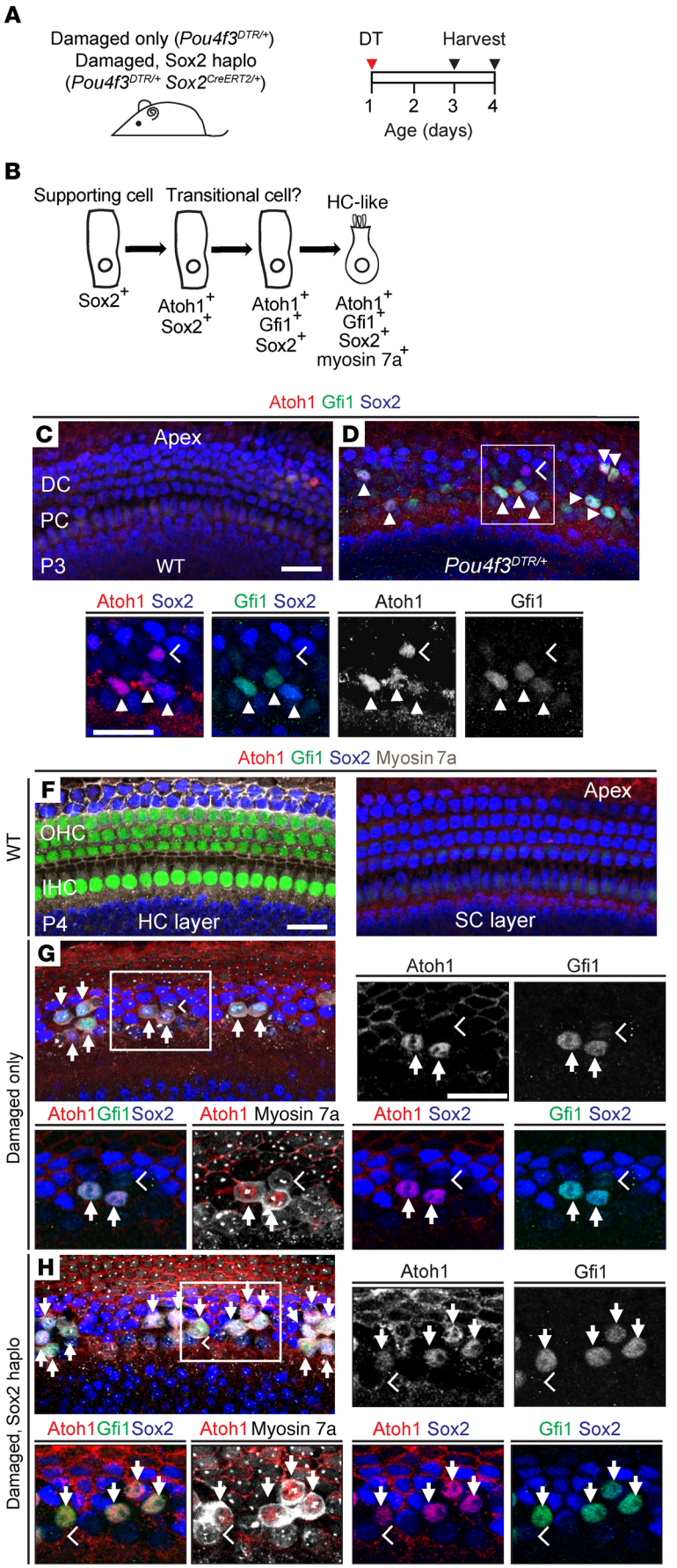

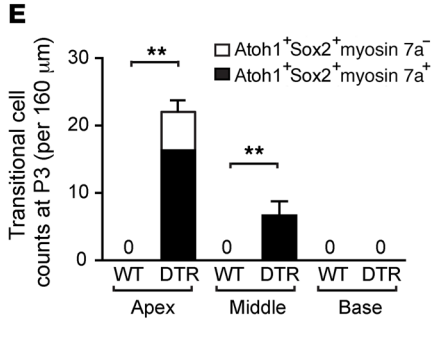

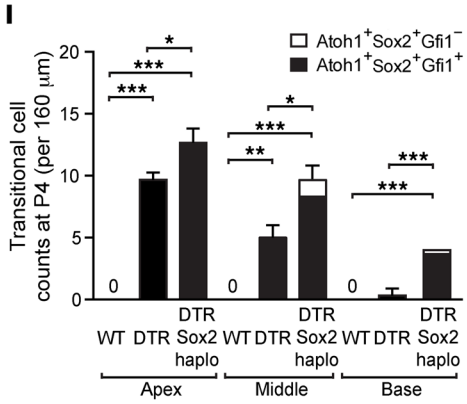

Figure 3. Sox2 reduction enhances transitional cell formation in the damaged neonatal mouse cochlea. (**A**) Schematic of hair cell ablation. P1 *Pou4f3*$^{DTR/+}$ and *Pou4f3*$^{DTR/+}$ *Sox2*$^{CreERT2/+}$ pups were injected with DT, and cochleae were examined on P3 and P4. (**B**) Cartoon depicts supporting cells forming transitional cells during regeneration. (**C**) Confocal images of P3 WT cochlea show no Atoh1 or Gfi1 expression in supporting cells. (**D**) After hair cell damage in the *Pou4f3*$^{DTR/+}$ cochlea, some Sox2$^+$ supporting cells expressed Atoh1 (chevrons) and Gfi1 (arrowheads), both early hair cell markers. All Gfi1$^+$Sox2$^+$ supporting cells expressed Atoh1, but some Atoh1$^+$Sox2$^+$ supporting cells did not express Gfi1. (**E**) Quantification of transitional cells (Atoh1$^+$Sox2$^+$ and Atoh1$^+$Sox2$^+$Gfi1$^+$) from WT and *Pou4f3*$^{DTR/+}$ cochleae. (**F**) P4 WT cochlea showed Gfi1 expression limited to hair cells and no Atoh1 or Gfi1 expression in Sox2$^+$ supporting cells. Atoh1 was absent in hair cells. (**G**) After DT-induced hair cell loss in *Pou4f3*$^{DTR/+}$ cochlea, Gfi1 was downregulated in the remaining myosin 7a$^+$ hair cells. Many transitional cells (arrows) (Atoh1$^+$Sox2$^+$myosin 7a$^+$Gfi1$^+$) were detected in all 3 cochlear turns. Like the P3 *Pou4f3*$^{DTR/+}$ cochlea, all transitional cells expressed Atoh1 and Sox2. In contrast to the P3 *Pou4f3*$^{DTR/+}$ cochlea, most transitional cells expressed myosin 7a by P4. Myosin7a+ cells with no expression of Sox2, Atoh1, or Gfi1 (chevron) likely represent surviving hair cells (**G** and **H**). (**H**) In the P4 *Pou4f3*$^{DTR/+}$ *Sox2*$^{CreERT2/+}$ cochlea, there were noticeably more transitional cells (arrows). (**I**) Quantification of transitional cells (Atoh1$^+$Sox2$^+$myosin 7a$^+$Gfi1$^+$ and Atoh1$^+$Sox2$^+$Gfi1$^+$) in WT, *Pou4f3*$^{DTR/+}$, and *Pou4f3*$^{DTR/+}$ *Sox2*$^{CreERT2/+}$ cochleae. Hair cell ablation led to a significantly greater number of transitional cells in each cochlear turn compared with that seen in controls. There were significantly more transitional cells detected in each turn of damaged, Sox2^{haplo} cochleae than in the damaged-only cochleae. The SD of transitional cell counts in the basal turn of damaged, Sox2^{haplo} cochleae is zero. Data represent the mean ± SD. $^*P < 0.05$, $^{**}P < 0.01$, and $^{***}P < 0.001$, by 1-way ANOVA with Holm-Sidak multiple comparisons test. $n = 3$. Scale bars: 20 μm.

There were, however, still significantly more hair cells in the Sox2^{haplo}, damaged cochleae than in the damaged-only cochleae. After DT administration, both *Pou4f3*$^{DTR/+}$ and *Pou4f3*$^{DTR/+}$ *Sox2*$^{CreERT2/+}$ animals showed markedly elevated auditory thresholds (Supplemental Figure 4G). Taken together, these results indicate that Sox2^{haplo} modestly promotes the survival of regenerated hair cells in the damaged cochlea, but the extent of survival is insufficient to establish auditory function.

Sox2^{haplo} enhances β-catenin–induced proliferation in the damaged neonatal cochlea. β-Catenin is the central mediator of the canonical Wnt signaling pathway, with exon 3 encoding a domain to be phosphorylated by glycogen synthase 3β. Phosphorylated β-catenin is degraded by the destruction complex, rendering the pathway inactive (52). In heterozygotes carrying β-catenin lacking exon 3, β-catenin is stabilized, leading to aberrant activation of Wnt signaling, and thus acts as a dominant mutation (53). Previous studies show that β-catenin stabilization in the neonatal cochlea causes proliferation and ectopic hair cell formation (54, 55). To further explore its role after damage, we first used 2 Cre-LoxP model systems to enhance Wnt signaling by stabilizing β-catenin in neonatal supporting cells (Figure 4, A and B). In *Fgfr3-iCre* mice given tamoxifen at P2, we detected Cre activity in approximately 86.9% of supporting cells in the P4 cochlea (using Ai14 tdTomato reporter mice; data not shown). To determine whether β-catenin stabilization enhances mitotic regeneration, we examined *Pou4f3*$^{DTR/+}$ *Fgfr3-iCre Ctnnb1*$^{fl(ex3)/+}$ (referred to hereafter as damaged, β-catenin^{GOF}) cochleae and compared them with damaged-only (*Pou4f3*$^{DTR/+}$) cochleae. We observed significantly more (~3.5-fold) EdU-labeled supporting cells and hair cells in the damaged, β-catenin^{GOF} cochleae, a finding that was limited to the apical turn (Figure 4, C–E, and I, and Supplemental Table 1). This suggests that β-catenin^{GOF} increases mitotic regeneration without expanding its domain to the middle or basal turns.

We next probed the effects of Sox2^{haplo} on β-catenin–induced mitotic regeneration by examining damaged, Sox2^{haplo}, β-catenin^{GOF} (*Pou4f3*$^{DTR/+}$ *Sox2*$^{CreERT2/+}$ *Ctnnb1*$^{fl(ex3)/+}$) cochleae. We found many EdU$^+$ supporting cells and hair cells in both the apical and middle turns and also observed EdU$^+$ supporting cells in the basal turn (Figure 4, F–I, and Supplemental Table 1). In comparison with the damaged, β-catenin^{GOF} cochlea, we observed an additional increase in the number of EdU$^+$ supporting cells and hair cells in the apical and middle turns (Figure 4I and Supplemental Table 1). Relative to the damaged, Sox2^{haplo} cochlea, the damaged, Sox2^{haplo}, β-catenin^{GOF} cochlea contained more EdU$^+$ supporting cells and hair cells in the apical turn only, while the cells in the middle and basal turns were not significantly different (Supplemental Table 1). These results indicate that both β-catenin^{GOF} and Sox2^{haplo} enhanced mitotic regeneration in the apical turn in the damaged cochlea. While Sox2^{haplo} extended the domain of mitotic regeneration into the middle and basal turns of the damaged cochlea, β-catenin^{GOF} failed to induce proliferation in this region, thus its mitogenic effect is spatially restricted to the apex.

Sox2^{haplo} acts as a permissive signal for β-catenin–responsive transitional cell formation in the damaged neonatal cochlea. To assess whether β-catenin^{GOF} also enhances transitional cell formation, we stained for Atoh1 and Gfi1 in the damaged, β-catenin^{GOF} cochlea (P4) and found transitional cells (Atoh1$^+$Gfi1$^+$Sox2$^+$) in the apical and middle turns (Figure 5, A, B, and D). However, we detected no transitional cells in the base (Figure 5F). Compared with damaged-only cochlea without stabilized β-catenin, fewer transitional cells expressed myosin 7a, although there was no significant change in the total number (Figure 5H and Supplemental Table 2), suggesting that β-catenin^{GOF} alone does not enhance transitional cell formation.

We next assessed whether Sox2^{haplo} affects β-catenin–induced transitional cell formation and examined damaged, Sox2^{haplo}, β-catenin^{GOF} cochleae. We detected a robust and significant increase in the number of transitional cells in all 3 cochlear turns compared with cell numbers in damaged, β-catenin^{GOF} or damaged-only (*Pou4f3*$^{DTR/+}$) cochleae (Figure 5, C, E, G, H, and Supplemental Table 2). Furthermore, to distinguish the effects of Sox2^{haplo} from those of β-catenin^{GOF}, we compared the effects and found that the number of transitional cells was significantly higher in damaged, Sox2^{haplo}, β-catenin^{GOF} cochleae than in damaged, Sox2^{haplo} cochleae without stabilized β-catenin (Supplemental Table 2). Taken together, these data suggest that both Sox2^{haplo} and damage act as permissive signals for β-catenin–induced transitional cell formation in the neonatal cochlea.

Sox2^{haplo} primes the neonatal cochlea for β-catenin–induced proliferation. We next probed the relationship between Sox2^{haplo} and β-catenin^{GOF} by examining the undamaged cochlea. After administering tamoxifen on P2 to β-catenin^{GOF} (*Fgfr3-iCre Ctnnb1*$^{(ex3)/+}$) mice, we did not detect any EdU-labeled supporting cells or ectopic hair cell formation in the P5 cochlea (Figure 6, A and B, and Supplemental Figure 5, A–C). However, after the same tamoxifen and EdU regimen, we found many EdU$^+$ supporting cells (but not hair cells) in the pillar cell region in the Sox2^{haplo}, β-catenin^{GOF} (*Sox2*$^{CreERT2/+}$ *Ctnnb1*$^{fl(ex3)/+}$) cochleae (Figure 6, A, C, and G, and Supplemental Figure 5, A, D, and E). To test whether cochlear supporting cells become β-catenin responsive upon acute downregulation of Sox2, we next concurrently stabilized β-catenin and partially deleted Sox2 by using *Fgfr3-iCre Sox2*$^{fl/+}$ *Ctnnb1*$^{fl(ex3)/+}$ (conditional Sox2^{haplo}, β-catenin^{GOF}) mice (Figure 6D and Supplemental Figure 5F) (32). As expected, no EdU$^+$ cells were detected in cochleae from β-catenin^{GOF} (*Fgfr3-iCre Ctnnb1*$^{fl(ex3)/+}$) mice given tamoxifen on P1 and EdU from P3 to P5 (Figure 6E, and Supplemental Figure 5, G, and H). This contrasts with the conditional Sox2^{haplo}, β-catenin^{GOF} (*Fgfr3-iCre Sox2*$^{fl/+}$ *Ctnnb1*$^{fl(ex3)/+}$) cochleae, in which we observed many EdU$^+$ supporting cells in the apical and middle turns (Figure 6, F and G, and Supplemental Figure 5, I and J).

To directly assess the effects of Sox2^{haplo} on Wnt signaling, we immunostained for the Wnt target Lef1 (56). In the P5 WT cochlea, we found that Lef1 expression was restricted to below the basilar membrane, where Wnt-responsive, tympanic border cells reside, as previously described (57), and we detected no expression in the sensory epithelium (Supplemental Figure 6, A–C). Similarly, we failed to detect Lef1 in the sensory epithelium from β-catenin^{GOF} or Sox2^{haplo} mice (Supplemental Figure 6, D–I). In the organ of Corti from Sox2^{haplo}, β-catenin^{GOF} cochlea, we found many Lef1$^+$ supporting cells in the apical turn, some of which were arranged as foci within the pillar cell region (Supplemental Figure 6, J–L). Thus Sox2^{haplo} acts as a permissive signal for β-catenin–induced Wnt activation in the undamaged, neonatal cochlea.

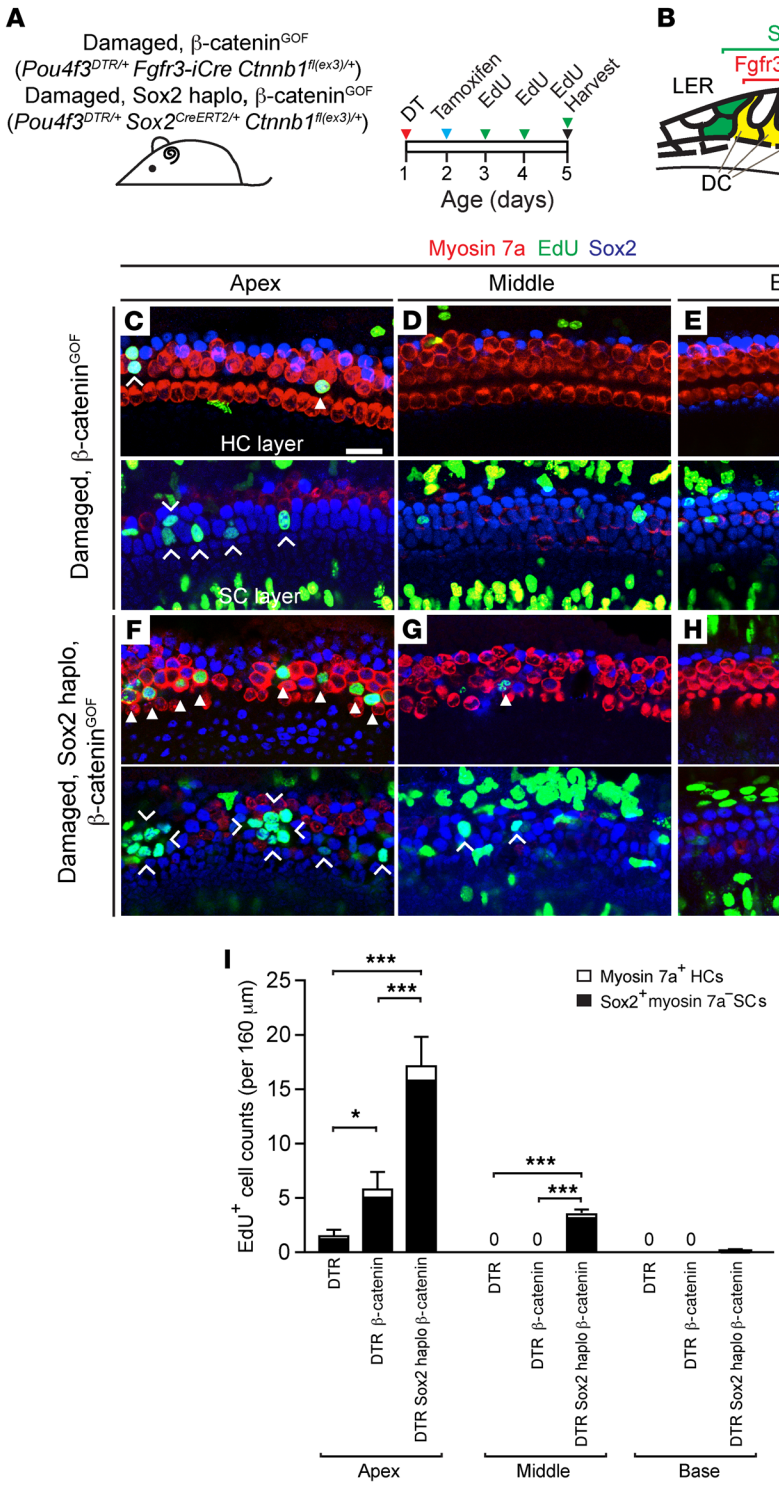

Figure 4. β-Catenin stabilization and Sox2 haploinsufficiency coordinate to increase mitotic regeneration in the damaged neonatal mouse cochlea. (**A**) *Pou4f3*$^{DTR/+}$ *Fgfr3-iCre Ctnnb1*$^{fl(ex3)/+}$ and *Pou4f3*$^{DTR/+}$ *Sox2*$^{CreERT2/+}$ *Ctnnb1*$^{fl(ex3)/+}$ pups were injected with DT on P1, tamoxifen on P2, and EdU daily (P3–P5), and cochleae were collected on P5. (**B**) Schematic depicting the domains of Fgfr3 and Sox2 expression in the neonatal mouse cochlea. (**C**–**E**) Confocal images of cochleae from P5 *Pou4f3*$^{DTR/+}$ *Fgfr3-iCre Ctnnb1*$^{fl(ex3)/+}$ mice showing EdU$^+$myosin 7a$^+$ hair cells (arrowhead) and EdU$^+$Sox2$^+$ supporting cells (chevrons) in the apical turn, but not in the middle or basal turn. Note that many EdU$^+$Sox2$^-$ cells resided outside the sensory epithelium. (**F**–**H**) In *Pou4f3*$^{DTR/+}$ *Sox2*$^{CreERT2/+}$ *Ctnnb1*$^{fl(ex3)/+}$ cochlea, there was a robust increase in the number of EdU$^+$myosin 7a$^+$ hair cells (arrowheads) and Sox2$^+$ supporting cells (chevrons) in the apical turn. As with *Pou4f3*$^{DTR/+}$ *Sox2*$^{CreERT2/+}$ cochlea, EdU$^+$ supporting cells were noted in the middle turns and occasionally in the basal turns. Many EdU$^+$Sox2$^-$ cells outside the sensory epithelium were also noted. (**I**) Quantification of EdU$^+$myosin 7a$^+$ hair cells and EdU$^+$Sox2$^+$ supporting cells in *Pou4f3*$^{DTR/+}$, *Pou4f3*$^{DTR/+}$ *Fgfr3-iCre Ctnnb1*$^{fl(ex3)/+}$, and *Pou4f3*$^{DTR/+}$ *Sox2*$^{CreERT2/+}$ *Ctnnb1*$^{fl(ex3)/+}$ cochleae. Data represent the mean ± SD. $^*P < 0.05$ and $^{***}P < 0.001$, by 1-way ANOVA with Holm-Sidak multiple comparisons test. $n = 3$–5. Scale bar: 20 μm.

We next immunostained for Atoh1 and Gfi1 to detect transitional cells in the undamaged, Sox2^{haplo}, β-catenin^{GOF} cochlea (*Fgfr3-iCre Sox2*$^{fl/+}$ *Ctnnb1*$^{fl(ex3)/+}$ and *Sox2*$^{CreERT2/+}$ *Ctnnb1*$^{fl(ex3)/+}$) (Figure 6H and Supplemental Figure 5K). We detected no Atoh1 expression and found that Gfi1 expression was confined to hair cells in cochleae subjected to β-catenin stabilization only (*Fgfr3-iCre Ctnnb1*$^{fl(ex3)/+}$) (Figure 6I and Supplemental Figure 5, L and M). Similarly, no transitional cells were found in the undamaged, Sox2^{haplo}, β-catenin^{GOF} cochleae from either model (Figure 6, J and K, and Supplemental Figure 5, N–Q). These data indicate that Sox2^{haplo} acts as a permissive signal for β-catenin–induced proliferation in the undamaged, neonatal cochlea. Moreover, we found that, in the absence of damage and Sox2^{haplo}, β-catenin^{GOF} does not induce transitional cell formation.

Sox2^{haplo} and β-catenin^{GOF} do not promote proliferation or hair cell formation in the mature cochlea. To test whether Sox2^{haplo} and β-catenin^{GOF} can induce regeneration in the damaged, mature cochlea, we used 2 models of hair cell ablation: aminoglycoside

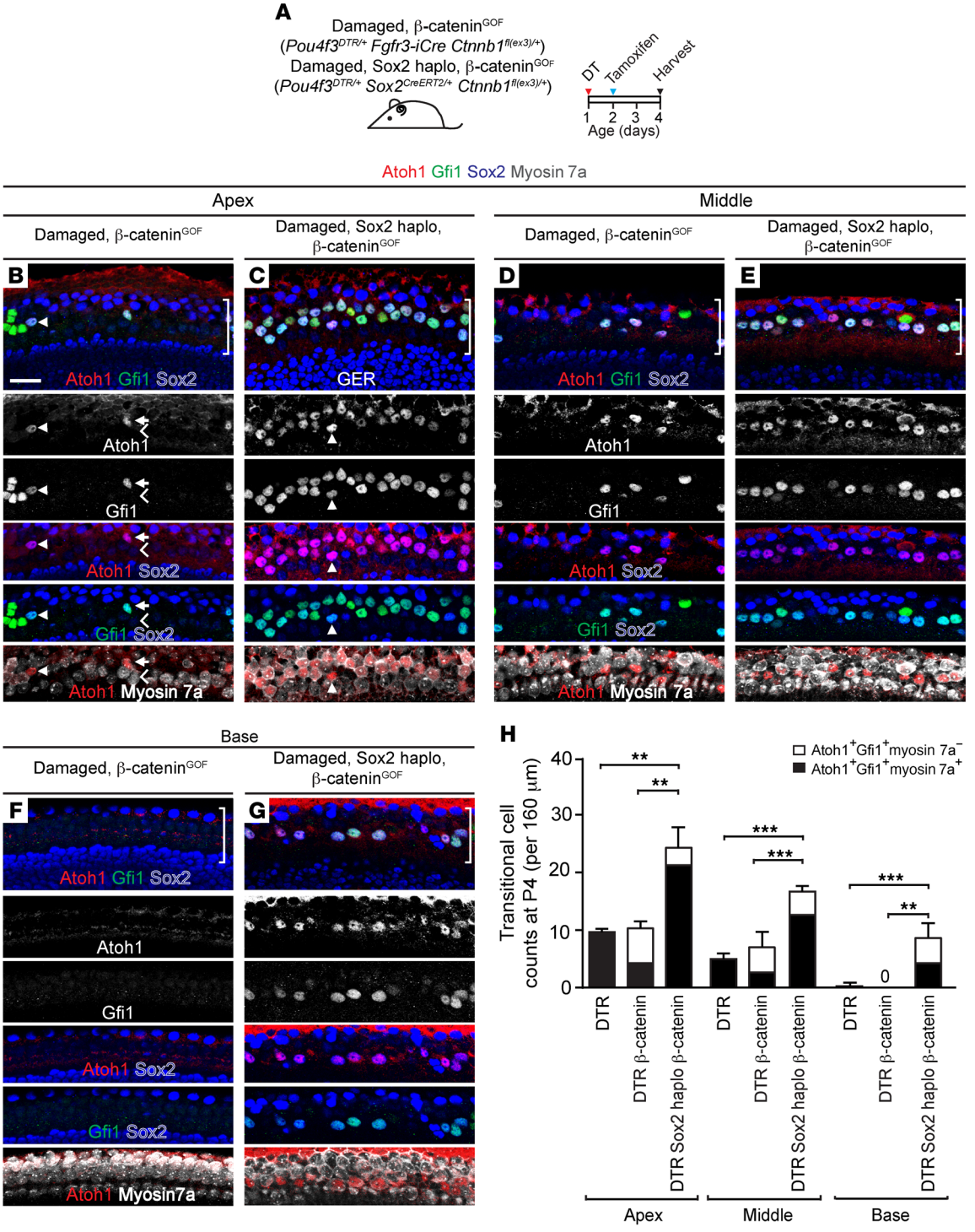

Figure 5. β-Catenin stabilization and Sox2 haploinsufficiency coordinate to increase transitional cell formation in the damaged neonatal mouse cochlea. (**A**) *Pou4f3*$^{DTR/+}$ *Fgfr3-iCre Ctnnb1*$^{fl(ex3)/+}$ and *Pou4f3*$^{DTR/+}$ *Sox2*$^{CreERT2/+}$ *Ctnnb1*$^{fl(ex3)/+}$ mice were injected with DT on P1, followed by tamoxifen administration on P2, and cochleae were examined on P4. (**B**, **D**, and **F**) As with *Pou4f3*$^{DTR/+}$ cochlea, some transitional cells (Atoh1$^+$Gfi1$^+$Sox2$^+$myosin 7a$^+$, arrows) were detected in the apical and middle turns of the *Pou4f3*$^{DTR/+}$ *Fgfr3-iCre Ctnnb1*$^{fl(ex3)/+}$ cochlea. Some Atoh1$^+$Gfi1$^+$Sox2$^+$ (myosin 7a$^-$) cells (arrowheads), which were rarely seen in the *Pou4f3*$^{DTR/+}$ cochlea, were also noted in the supporting cell layer of apical and middle turns. Some myosin 7a$^+$Atoh1$^-$Gfi1$^-$ hair cells (chevrons) were also observed in all 3 turns and were presumed to be surviving hair cells. (**C**, **E**, and **G**) In the *Pou4f3*$^{DTR/+}$ *Sox2*$^{CreERT2/+}$ *Ctnnb1*$^{fl(ex3)/+}$ cochlea, a marked increase in transitional cells was observed in all 3 turns. (**H**) Quantification revealed that significantly more transitional cells were detected in all 3 turns in the *Pou4f3*$^{DTR/+}$ *Sox2*$^{CreERT2/+}$ *Ctnnb1*$^{fl(ex3)/+}$ cochleae than in either *Pou4f3*$^{DTR/+}$ or *Pou4f3*$^{DTR/+}$ *Fgfr3-iCre Ctnnb1*$^{fl(ex3)/+}$ cochleae. Data represent the mean ± SD. $^{**}P < 0.01$ and $^{***}P < 0.001$, by 1-way ANOVA with Holm-Sidak multiple comparisons test. $n = 3$. Scale bar: 20 μm.

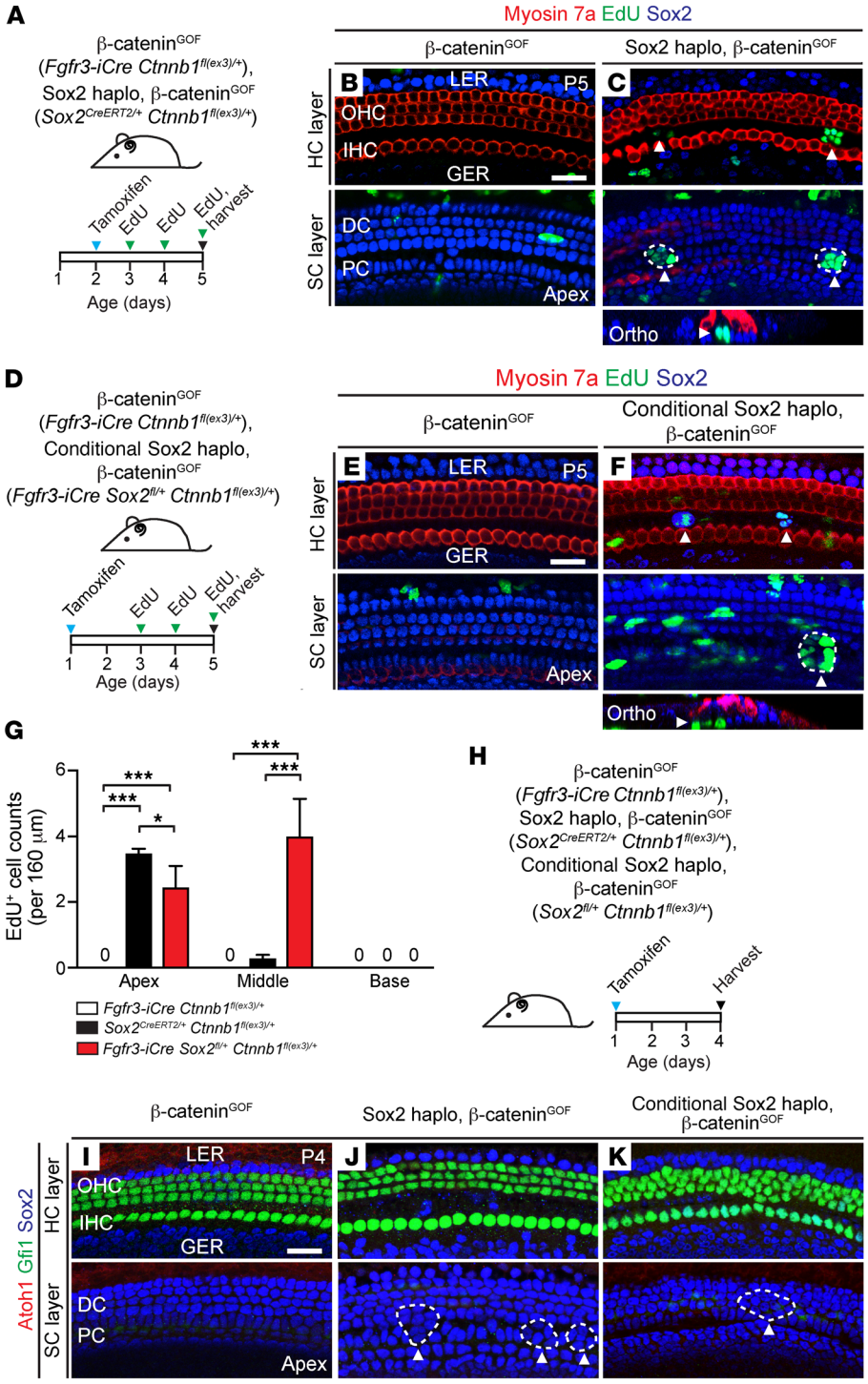

Figure 6. Sox2 haploinsufficiency acts as a permissive signal for β-catenin–induced proliferation in the undamaged neonatal cochlea. (**A**) Schematic of the experimental paradigm. *Fgfr3-iCre Ctnnb1*$^{fl(ex3)/+}$ and *Sox2*$^{CreERT2/+}$ *Ctnnb1*$^{fl(ex3)/+}$ pups were given tamoxifen on P2, followed by daily administration of EdU (P3–P5), and cochleae were examined on P5. (**B**) No EdU$^+$ cells were detected in the organ of Corti in cochleae from *Fgfr3-iCre Ctnnb1*$^{fl(ex3)/+}$ mice treated with tamoxifen on P2. (**C**) EdU$^+$ supporting cells but not hair cells arranged as foci (dashed lines, arrowhead) were found in P5 *Sox2*$^{CreERT2/+}$ *Ctnnb1*$^{fl(ex3)/+}$ cochleae. (**D**) *Fgfr3-iCre Ctnnb1*$^{fl(ex3)/+}$ and *Fgfr3-iCre Sox2*$^{fl/+}$ *Ctnnb1*$^{fl(ex3)/+}$ pups were given tamoxifen on P1, followed by EdU administration daily (P3–P5), and cochleae were examined on P5. (**E**) The apical turn of *Fgfr3-iCre Ctnnb1*$^{fl(ex3)/+}$ cochleae revealed no EdU$^+$ hair cells or supporting cells. (**F**) Like *Sox2*$^{CreERT2/+}$ *Ctnnb1*$^{fl(ex3)/+}$ cochlea, but in contrast to *Fgfr3-iCre Ctnnb1*$^{fl(ex3)/+}$ cochlea, EdU$^+$ cells arranged as clusters (dashed lines, arrowheads) were found in *Fgfr3-iCre Ctnnb1*$^{fl(ex3)/+}$ *Sox2*$^{fl/+}$ cochlea (tamoxifen was given on P1). (**G**) Quantification of EdU$^+$ cells. The differences in EdU$^+$ cells between Sox2^{haplo} and conditional Sox2^{haplo} models can be attributed to the timing or degrees of Sox2 partial deletion. (**H**) *Fgfr3-iCre Ctnnb1*$^{fl(ex3)/+}$, *Sox2*$^{CreERT2/+}$ *Ctnnb1*$^{fl(ex3)/+}$, and *Fgfr3-iCre Sox2*$^{fl/+}$ *Ctnnb1*$^{fl(ex3)/+}$ pups were injected with tamoxifen on P1, and cochleae were harvested on P4. (**I**) Gfi1-labeled hair cells were present, but no Atoh1- or Gfi1-labeled Sox2$^+$ supporting cells were detected in *Fgfr3-iCre Ctnnb1*$^{fl(ex3)/+}$ cochlea. (**J**) No Atoh1- or Gfi1-labeled Sox2$^+$ supporting cells were detected in *Sox2*$^{CreERT2/+}$ *Ctnnb1*$^{fl(ex3)/+}$ cochlea, although foci-like clusters were still noted in the pillar cell region (dashed lines, arrowheads). (**K**) Neither Atoh1- nor Gfi1-labeled transitional cells were detected in *Fgfr3-iCre Ctnnb1*$^{fl(ex3)/+}$ *Sox2*$^{fl/+}$ cochlea (tamoxifen was administered on P1), although foci-like clusters could still be observed (dashed line, arrowhead). Data represent the mean ± SD. $^*P < 0.05$ and $^{***}P < 0.001$, by 1-way ANOVA with Holm-Sidak multiple comparisons test. $n = 3$. Scale bars: 20 μm.

(AG) (sisomicin with furosemide) (58) and DT (44) treatment (Figure 7A and Supplemental Figure 7A). After drug administration on P21, both damage paradigms led to significant hair cell loss by P28 (Figure 7, B–E). AGs caused primarily outer hair cell loss, and DT (*Pou4f3*$^{DTR/+}$) caused mainly inner hair cell loss. Both damage models showed significantly elevated ABR thresholds, with the AG model also showing higher DPOAE thresholds (Figure 7, F and G).

To test the effects of Sox2^{haplo} and β-catenin^{GOF} on damaged, mature cochlea, we examined the *Fgfr3-iCre Ctnnb1*$^{fl(ex3)/+}$ and *Sox2*$^{CreERT2/+}$ *Ctnnb1*$^{fl(ex3)/+}$ mice (β-catenin^{GOF} alone and Sox2^{haplo} and β-catenin^{GOF}, respectively) (Figure 7H). Cochleae from *Fgfr3-iCre* (damaged only) and *Sox2*^{CreERT2} (damaged, Sox2^{haplo}) mice served as controls. Tamoxifen administration on P22 led to approximately 70.8% ± 14.9% Cre$^+$ supporting cells in *Fgfr3-iCre Rosa26*$^{tdTomato/+}$ cochleae (data not shown) and a decrease of 30.0% ± 18.1% in *Ctnnb1* exon 3 mRNA levels in whole *Fgfr3-iCre Ctnnb1*$^{fl(ex3)/+}$ cochleae (Figure 7I), suggesting that activated Cre recombinase and β-catenin were effectively modified for stabilization.

In the AG- and DT-damaged cochleae, we detected no EdU-labeled cells within the organ of Corti in the β-catenin^{GOF} or Sox2^{haplo},

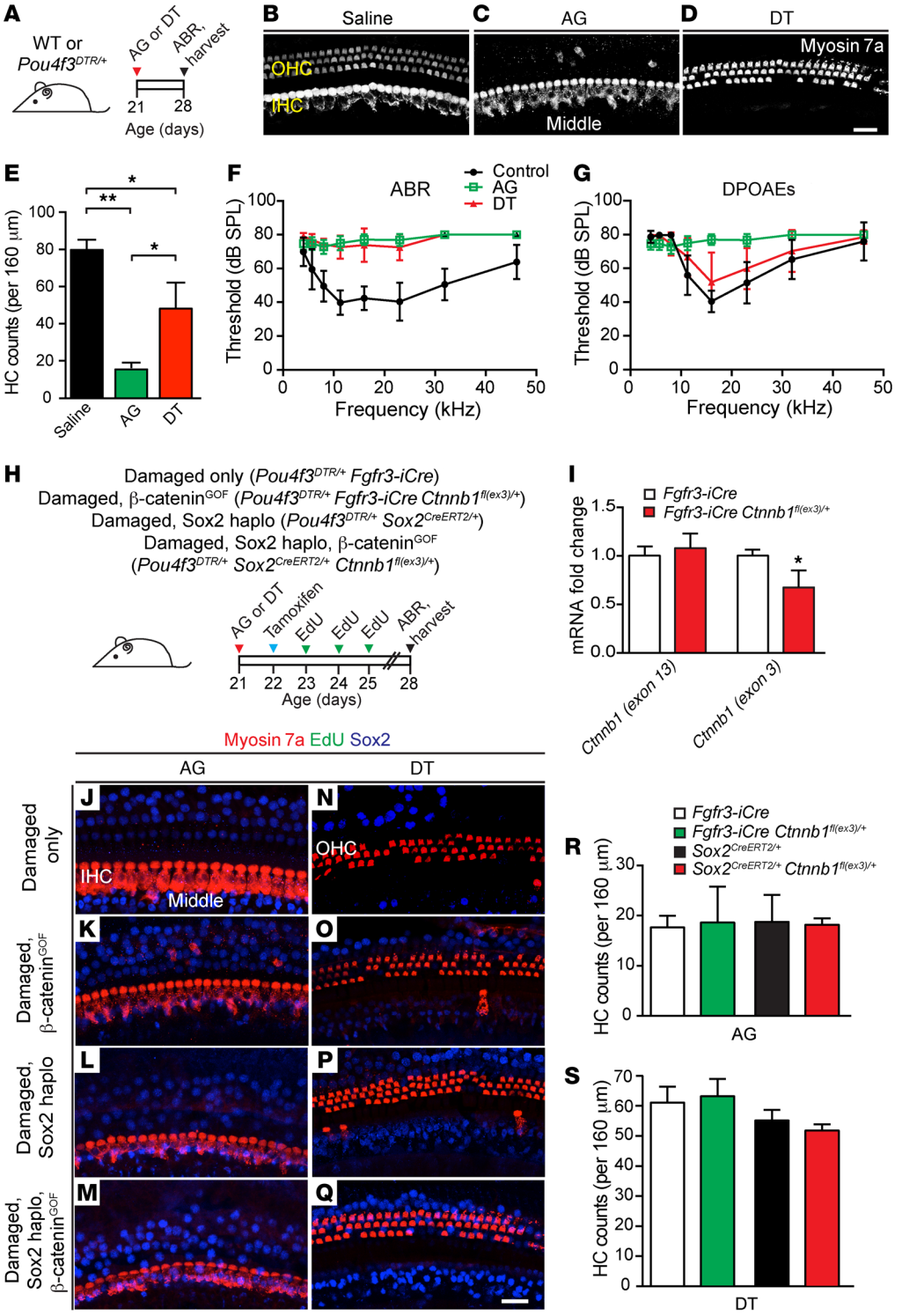

Figure 7. Sox2 haploinsufficiency and β-catenin stabilization do not induce mitotic hair cell regeneration in the damaged adult cochlea. (**A**) Schematic showing the use of AG (sisomicin combined with furosemide) or DT to damage the mature cochlea in WT and *Pou4f3*$^{DTR/+}$ mice. (**B**–**D**) Saline-treated mice containing a full complement of myosin 7a$^+$ cochlear inner hair cells and outer hair cells. A loss of outer hair cells after AG treatment and of inner hair cells after DT treatment was observed. Some outer hair cell loss after DT treatment was observed. (**E**) Quantification revealed a significant decrease in hair cell numbers in both damage paradigms. (**F** and **G**) ABR thresholds were significantly higher in both the AG- and DT-treated animals as compared with controls. A significant threshold shift was also observed in the DPOAEs in AG-treated animals, but not in the animals treated with DT. (**H**) Schematic of transgenic mouse models and experimental timeline. Cochleae were damaged on P21, tamoxifen was given on P22, followed by EdU administration from P23 to P25, and the animals were sacrificed after ABR on P28. (**I**) qPCR showing a significant reduction of *Ctnnb1* (exon3) mRNA expression but not of *Ctnnb1* (exon 13) mRNA expression in cochleae from *Fgfr3-iCre Ctnnb1*$^{fl(ex3)/+}$ mice. (**J**–**M**) No EdU$^+$Sox2$^+$ supporting cells or myosin 7a$^+$ hair cells were detected after AG treatment in any of the genotypes examined. A persistent loss of outer hair cells was seen in these cochleae, without any new Sox2$^+$myosin 7a$^+$ hair cells. (**N**–**Q**) There were no EdU$^+$ hair cells or supporting cells after DT treatment or formation of new Sox2$^+$myosin 7a$^+$ hair cells in any of the mouse cohorts. (**R** and **S**) Quantification of hair cells in AG- and DT-treated cochleae showing no change in hair cell numbers among genotypes. Data represent the mean ± SD. *$P < 0.05$ and **$P < 0.01$, by 2-tailed Student's *t* test or 1-way ANOVA with Holm-Sidak multiple comparisons test. n = 3–11. Scale bars: 20 μm.

β-catenin^{GOF} cochleae 1 week after damage (Figure 7, J–Q, and Supplemental Figure 7, B–Q), nor did we detect any EdU-labeled cells within the organ of Corti 3 weeks after damage (data not shown). Moreover, BrdU administered via the drinking water for 2 weeks (P23–P37) to AG-damaged *Fgfr3-iCre Ctnnb1*$^{fl(ex3)/+}$ mice also failed to label cells in the organ of Corti (Supplemental Figure 7, V–X). To assess for transitional cell formation, we immunostained cochleae from AG-treated, Sox2^{haplo}, β-catenin^{GOF} (*Sox2*$^{CreERT2/+}$ *Ctnnb1*$^{fl(ex3)/+}$) mice and found no Atoh1^{+} supporting cells 4 days after damage (not shown). In addition, myosin 7a^{+} hair cell counts did not differ among the 4 groups: (a) damaged-only control cochleae, (b) damaged and Sox2^{haplo} cochleae, (c) damaged and β-catenin^{GOF} cochleae, and (d) damaged, Sox2^{haplo}, β-catenin^{GOF} cochleae) 1 week (Figure 7, R and S) or 3 weeks after damage (data not shown). Lastly, ABR and DPOAE measurements revealed no differences in thresholds among damaged-only, damaged and β-catenin^{GOF}, and damaged, Sox2^{haplo}, β-catenin^{GOF} animals 3 weeks after damage (Supplemental Figure 7, R–U). Thus, our data indicate that supporting cells in the damaged, mature cochlea are not competent to divide or form transitional cells in response to Sox2^{haplo} and/or β-catenin^{GOF}.

Downstream targets of Sox2 haploinsufficiency. Our results so far suggest that Sox2^{haplo} acts as a permissive signal for supporting cells to proliferate, form transitional cells, and be responsive to β-catenin in the damaged, neonatal cochlea but not in the damaged, mature cochlea. To gain insights into possible mechanisms governing this phenomenon, we measured mRNA expression of Notch (*Hes5*, *Hes1*, and *Hey1*) and Wnt (*Axin2*, *Lef1*, and *Lgr5*) target genes in 4 groups of cochleae from P5 and P25 mice: (a) undamaged WT; (b) undamaged, Sox2^{haplo} (*Sox2*$^{CreERT2/+}$); (c) damaged only (*Pou4f3*$^{DTR/+}$); and (d) damaged, Sox2^{haplo} (*Pou4f3*$^{DTR/+}$ *Sox2*$^{CreERT2/+}$) (Figure 8A and Supplemental Figure 8A).

Both the neonatal and mature Sox2^{haplo} cochleae expressed significantly lower levels of *Sox2* (23.1% ± 11.1% and 42.7% ± 29.2%, respectively) when compared with levels in WT tissues (Figure 8, B and C). We also detected a significant reduction in *Sox2* levels in the damaged-only (*Pou4f3*$^{DTR/+}$, 29.1% ± 16.7%) cochleae and damaged, Sox2^{haplo} (*Pou4f3*$^{DTR/+}$ *Sox2*$^{CreERT2/+}$, 21.4% ± 6.1%) cochleae compared with levels in WT control cochleae (Figure 8B). By contrast, *Sox2* levels did not significantly change after damage in the mature cochlea (Figure 8C).

Neonatal cochleae from *Sox2*$^{CreERT2/+}$ mice had a significant reduction in levels of the Notch target gene *Hes5* (47.8% ± 29.9%) relative to levels in WT control cochleae (Figure 8D). This decrease was also detected using semiquantitative in situ experiments on sections from *Sox2*$^{CreERT2/+}$ and WT cochleae (Supplemental Figure 9, A–F). After DT damage alone (*Pou4f3*$^{DTR/+}$) or when combined with Sox2^{haplo} (*Pou4f3*$^{DTR/+}$ *Sox2*$^{CreERT2/+}$), we also observed a significant decrease in *Hes5* expression (25.4% ± 10.3% and 31.3% ± 10.6%, respectively) (Figure 8D). However, no change in *Hes5* expression was detected in the mature cochlea (Figure 8E). Moreover, we observed no changes in the levels of expression of other Notch target genes (*Hes1* and *Hey1*) in the neonatal or mature cochleae (Supplemental Figure 8, B–E). We also found no significant changes in the expression of Wnt target genes (*Axin2*, *Lgr5*, and *Lef1*) in the 4 groups of neonatal and mature cochleae examined (Supplemental Figure 8, F–K). These results suggest that decreased expression in components of the Notch pathway may mediate the permissive signals conferred by Sox2^{haplo} or damage to induce proliferation, the formation of transitional cells, and responsiveness to β-catenin^{GOF}.

Discussion

Sox2 directs the cell cycle and cell fate during the development of diverse tissue types. Complete and partial Sox2 deficiencies cause multiorgan defects including anophthalmia, epilepsy, and trachea-esophageal, cochlear, and genital anomalies in mice and humans (10, 11, 17–20). Moreover, some regenerating tissues are sensitive to Sox2 dosage and are dependent on Sox2 activation (10, 17, 27). Our study shows that Sox2 haploinsufficiency allows essentially normal development of the cochlea. Furthermore, in contrast to the previous notion that Sox2 upregulation promotes tissue regeneration, Sox2 haploinsufficiency primes the cochlea to regenerate in vivo.

Competence and domains of tissue regeneration. In the avian cochlea, 2 mechanisms mediate hair cell regeneration in distinct regions of the organ: nonmitotic, direct transdifferentiation in the abneural region and mitotic regeneration in the neural domain (59). While the mature mammalian cochlea does not regenerate, fate-mapping studies demonstrate that supporting cells in the neonatal cochlea spontaneously proliferate and form new hair cells after damage (43, 45). Cox and colleagues showed that proliferation primarily occurred in the apical region, while the fate-mapped, immature hair cells were present in all 3 turns of the neonatal cochlea. Given the results of these studies, we hypothesized that proliferation competence and phenotypic conversion (which we characterize as transitional cell formation) are distinct and differentially regulated.

Several findings in our study support the notion that cell proliferation and transitional cell formation are differentially governed. First, while mitotic cells in the Sox2^{haplo} cochlea mainly resided in the apical turn, we found ectopic hair cells in all 3 cochlear turns. After damage, mitotic regeneration occurred primarily in the apical turn, with transitional (Atoh1^{+}) cell formation observed more broadly in the apical and middle turns (Figure 8F). Thus, as with Sox2^{haplo}, damage confers competence in supporting cells to both proliferate and form transitional cells. Moreover, the effects of Sox2^{haplo} and damage appear additive in conferring to supporting cells the competence to mitotically regenerate and form transitional cells. Building on previous studies showing that Sox2 antagonizes hair cell specification in the embryonic cochlea (11) and inhibits proliferation (60), the current results unveil roles for Sox2^{haplo} as a positive modulator of mitotic hair cell regeneration and transition cell formation in the damaged postnatal cochlea. However, Sox2 is required during hair cell regeneration in the zebrafish inner ear (61), and whether Sox2 is similarly indispensable during mammalian hair cell regeneration remains to be determined.

Competence to respond to Wnt activation. In contrast to previous studies (54, 55), our results indicate that postnatal cochlear supporting cells in a resting, undamaged state are not competent to proliferate or form ectopic hair/transitional cells upon Wnt activation. Rather, damage or Sox2^{haplo} confers to supporting cells the competence to proliferate in response to Wnt activation. Further, the competence to form additional transitional cells in response to Wnt activation requires the presence of both

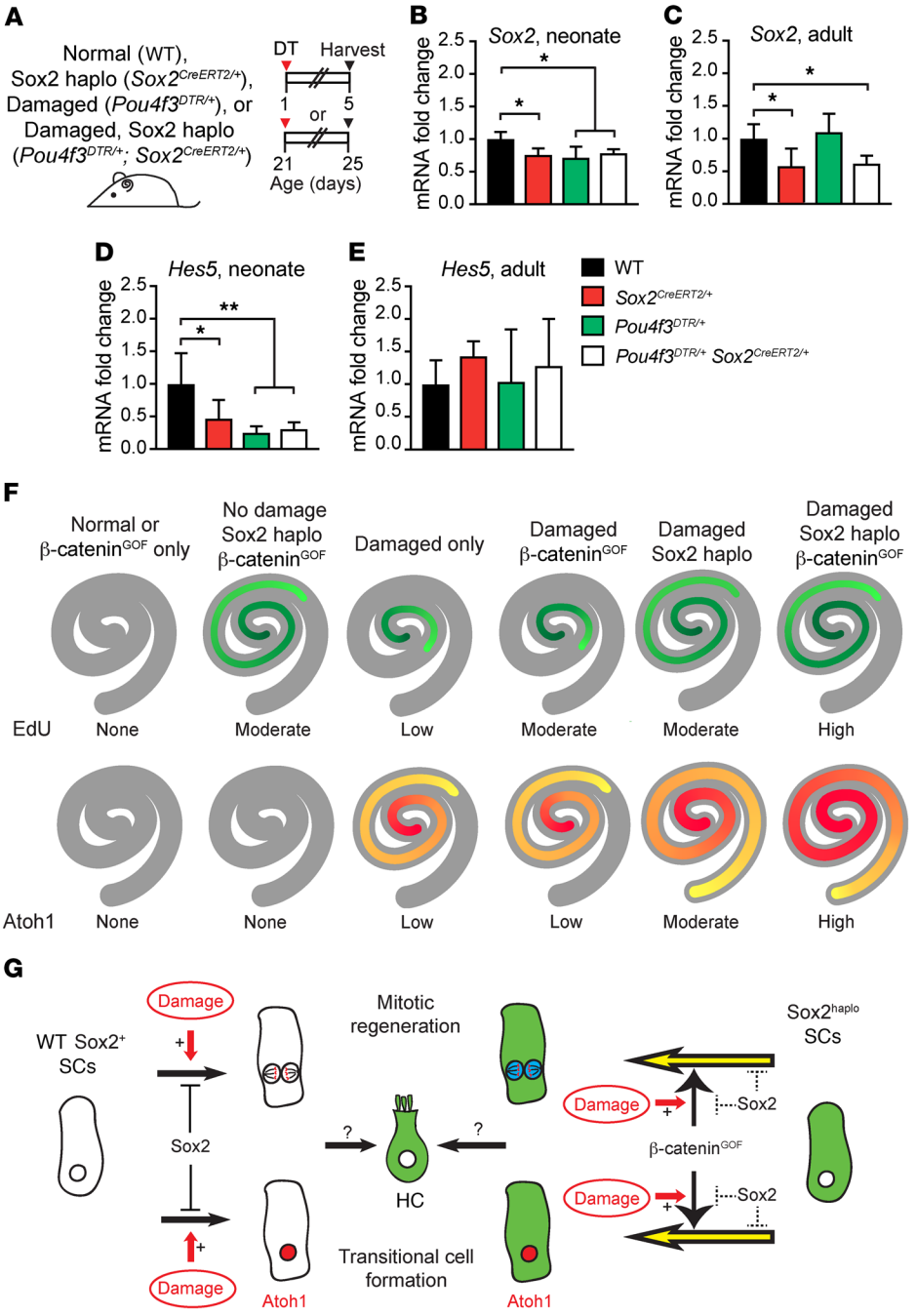

Figure 8. qPCR of Notch and Wnt target genes in damaged and Sox2-haplo-insufficient cochleae. (**A**) Neonatal (P1) and mature (P21) WT, *Sox2*$^{CreERT2/+}$, *Pou4f3*$^{DTR/+}$, and *Pou4f3*$^{DTR/+}$ *Sox2*$^{CreERT2/+}$ mice were treated with DT, and cochleae were collected 4 days later. (**B**) A significant decrease was detected in *Sox2* expression levels in the neonatal *Sox2*$^{CreERT2/+}$, *Pou4f3*$^{DTR/+}$, and *Pou4f3*$^{DTR/+}$ *Sox2*$^{CreERT2/+}$ cochleae relative to levels in WT controls. (**C**) Only the mature *Sox2*$^{CreERT2/+}$ and *Pou4f3*$^{DTR/+}$ *Sox2*$^{CreERT2/+}$ cochleae had lower *Sox2* levels than those detected in control cochleae. (**D**) A significant decrease in the levels of the Notch target gene *Hes5* was detected in *Sox2*$^{CreERT2/+}$, *Pou4f3*$^{DTR/+}$, and *Pou4f3*$^{DTR/+}$ *Sox2*$^{CreERT2/+}$ cochleae relative to levels in WT cochleae on P5. (**E**) When measured on P25, no significant changes in the expression levels of *Hes5* were seen relative to WT cochleae. Expression levels of *Sox2* and *Hes5* in the mature WT cochleae were lower than levels in P5 WT cochleae. (**F**) Schematics depicting the extent and patterns of proliferation and Atoh1^{+} transitional cells under various defined conditions. Darker colors represent more robust proliferation or the formation of transitional cells. (**G**) Proposed model of Sox2 and damage coordination in regulating mitotic regeneration, transitional cell formation, and Wnt responsiveness. $^{*}P < 0.05$ and $^{**}P < 0.01$, by 1-way ANOVA with Holm-Sidak multiple comparisons test. $n = 4$.

damage and Sox2^{haplo}. These findings lend additional evidence for the differential regulation of mitotic regeneration and transitional cell formation.

While the context-dependent effects of Wnt activation are known (62), the mechanisms dictating the permissiveness to respond to β-catenin activation remain poorly understood. A potential mechanism is the differential inhibition of Wnt signaling, a finding noted in intestinal polyposis and hepatic carcinogenesis (63). Several Sox family transcription factors directly interact with β-catenin to repress Wnt transcriptional responses, while others can enhance Wnt target gene expression (64). Sox2 represses proliferation in Wnt-driven gastric adenoma formation (65) and cancer (66), but in other contexts such as breast cancer, it stimulates β-catenin–induced proliferation (67). This study posits a model in which Sox2 represses the mitogenic and prosensory effects of β-catenin activation, possibly via activation of the Notch signaling effector Hes5. Although we did not detect a significant change in defined Wnt target genes in Sox2^{haplo} or damaged cochleae, it is also possible that decreased Sox2 expression causes a small degree of disinhibition of Wnt signaling and directly facilitates the effects induced by β-catenin stabilization. In support of our finding of Notch signaling involvement, Sox2 regulates retinal progenitor cell proliferation/differentiation in a dose-dependent manner via Notch signaling (10). Moreover, Notch1 deletion enhances β-catenin–induced mitotic generation of hair cells in the neonatal cochlea (68). Like Sox2, *Hes5* suppresses Atoh1 during cochlear development (69, 70),

and Notch inhibition increases Atoh1 expression and hair cell formation in undamaged (71–73) and damaged neonatal cochleae (74).

In the postnatal cochlea, *Hes5* is highly expressed in Sox2$^+$ supporting cells and becomes downregulated in the mature cochlea (75–77). The most notable difference between the neonatal and mature cochleae is that the former had lower expression of *Hes5* as a result of Sox2^{haplo} or damage. By contrast, *Hes5* and other Notch target genes were expressed at low levels and were not altered as a result of Sox2^{haplo} or damage in the mature cochlea, suggesting that they play a significant role in restricting hair cell regeneration in the neonatal, but not the mature cochlea. Thus, Sox2^{haplo} and damage may coordinate to dictate mitotic regeneration, transitional cell formation, and Wnt responsiveness via Notch signaling in the neonatal cochlea, but not in the mature cochlea (Figure 8G) because of age-related changes of these factors. Our results are in agreement with previous reports noting a decline of *Hes5* expression in the maturing cochlea (72, 75). Furthermore, *Hes5* and *Atoh1* expression remained low in the noise-damaged mature cochlea (77). Another important consideration is the largely unknown network of transcription factors that act in concert with Sox2 and Hes5 in the neonatal and mature cochlea. Moreover, gene silencing by epigenetic factors occurs as the cochlea develops and matures (78), thus a more comprehensive investigation in these areas, including further study of the roles of Hes5, should be of interest and may help guide future therapy using Sox2 and Wnt signaling to regenerate the mature cochlea.

Mouse models to study regeneration. The results of this study underscore the potential confounding effects from haploinsufficiency when using knockin mouse models (79). For example, the Foxg1-Cre mouse line can have brain deficits that probably stem from alterations in proliferation, possibly as a result of haploinsufficiency (80–82). In the same vein, the differences between our results and those of previous studies, in which β-catenin stabilization induced proliferation in the nondamaged neonatal cochlea, can be attributed to the knockin mouse lines used (*Sox2*$^{CreERT2/+}$ and *Lgr5*$^{CreERT2/+}$) (54, 55). Moreover, the proliferative cells observed after β-catenin stabilization in Lgr5$^+$ cells in the neonatal cochlea may have originated from inner phalangeal cells medial to the inner hair cells. While the robust proliferation observed in the neonatal *Sox2*$^{CreERT2/+}$ cochlea is affected by Sox2 haploinsufficiency (55, 68, 83), one should also consider the differences in experimental paradigms used and the supporting cell subtypes examined.

In summary, our results introduce a model system for mammalian hair cell regeneration, in which Sox2 haploinsufficiency enhances regeneration, and reveal the cooperative roles between Sox2 haploinsufficiency and damage in governing mitosis, differentiation, and Wnt responsiveness of hair cell precursors in the neonatal cochlea, probably via components of Notch signaling. These findings illustrate the differential responsiveness of cochlear supporting cells as hair cell progenitors in resting and damaged states. Moreover, these findings demonstrate the possibility of priming supporting cells, without hindering their normal function, to enhance their regenerative ability in response to damage and/or adjuvant therapy such as Wnt activation. Thus, this study should provide insights that will help guide the future design of combinatorial approaches for stimulating mammalian cochlear regeneration to reverse hearing loss.

Methods

Mice. The following mouse strains were used: *Sox2*$^{fl/+}$ (The Jackson Laboratory; stock 13093) (84); *Fgfr3-iCre* (gift of W. Richardson, Wolfson Institute for Biomedical Research, University College London, London, United Kingdom) (85); *R26R*$^{tdTomato/+}$ (The Jackson Laboratory; stock 7914) (86); *Ctnnb1*$^{fl(ex3)/+}$ (gift of M. Taketo, Kyoto University, Kyoto, Japan) (53); *Sox2*$^{GFP/+}$ (The Jackson Laboratory; stock 17592) (21); *Pou4f3*$^{DTR/+}$ (gift of E. Rubel, Department of Otolaryngology – Head and Neck Surgery, University of Washington, Seattle, Washington, USA) (44); Sox2$^{CreERT2/+}$ (The Jackson Laboratory; stock 17593) (21); and *Atoh1*$^{GFP/+}$ (The Jackson Laboratory; stock 13593) (50). Mice of both sexes were used. To induce Cre recombinase activity, tamoxifen (dissolved in corn oil; MilliporeSigma) was injected i.p. into neonatal (0.075 mg/g) and adult (0.225 mg/g) mice. In neonatal mice, hair cell loss was induced on P1 by i.p. administration of DT (6.25 ng/g; MilliporeSigma). In WT mice, damage was induced on P21 by a combined treatment with the AG sisomicin sulfate (i.p., 200 mg/kg; OChem) and the loop diuretic furosemide (i.p., 300 mg/kg; Novaplus) (58). P21 *Pou4f3*$^{DTR/+}$ mice were administered DT (i.p., 6.25 mg/kg), EdU (i.p., 25 mg/kg; Invitrogen, Thermo Fisher Scientific), or BrdU (1 mg/ml in the drinking water; Invitrogen, Thermo Fisher Scientific).

Genotyping and qPCR. A genomic DNA template was produced by adding 180 μl of 50 mM NaOH to tissue biopsies and incubating at 98°C for 1 hour, at which point 20 μl of 1 M Tris-HCl was added. The primers used were as follows: Cre mutant, forward (5′-GCGGTCTGCCAGTAAAAACTATC-3′), Cre mutant, reverse (5′-GTGAAACAGCATTGCTGTCACTT-3′); Cre WT, forward (5′-CTAGGCCACAGAATTGAAAGATCT-3′), Cre WT, reverse (5′-GTAGGTGGAAATTCTAGCATCC-3′); *Ctnnb1*$^{fl(ex3)/+}$, forward (5′-AAGGTAGAGTGATGAAAGTTG-3′), *Ctnnb1*$^{fl(ex3)/+}$, reverse (5′-CACCATGTCCTCTGTCTATTC-3′); *Fgfr3-iCre*, forward (5′-GAGGGACTACCTCCTGTACC-3′) and *Fgfr3-iCre*, reverse (5′-TGCCCAGACTCATCCTTGGC-3′); *R26R*$^{tdTomato/+}$ mutant, forward (5′-CTGTTCCTGTACGGCATGG-3′), *R26R*$^{tdTomato/+}$ mutant, reverse (5′-GGCATTAAAGCAGCGTATCC-3′); *R26R*$^{tdTomato/+}$ WT, forward (5′-AAGGGAGCTGCAGTGGAGTA-3′), *R26R*$^{tdTomato/+}$ WT, reverse (5′-CCGAAAATCTGTGGGAAGTC-3′); *Pou43f*$^{DTR/+}$, forward (5′-GTCAAAAAATGTGCCTTAGAGCGG-3′), *Pou4f3*$^{DTR/+}$, reverse (5′-CCGACGGCAGCAGCTTCATGGTC-3′); *Pou4f3*$^{DTR/+}$ WT, forward (5′-CACTTGGAGCGCGGAGAGCTAG-3′), *Pou4f3*$^{DTR/+}$ reverse (5′-CCGACGGCAGCAGCTTCATGGTC-3′); *Sox2*$^{fl/+}$, forward (5′-TGGAATCAGGCTGCCGAGAATCC-3′), *Sox2*$^{fl/+}$, reverse (5′-TCGTTCTGGCAACAAGTGCTAAAGC-3′); *Sox2*$^{GFP/+}$ mutant, forward (5′-AAGTTCATCTGCACCACCG-3′), *Sox2*$^{GFP/+}$ mutant, reverse (5′-TCCTTGAAGAAGATGGTGCG-3′); *Sox2*$^{GFP/+}$ WT, forward (5′-CGTGATCTGCAACTCCAGTC-3′), *Sox2*$^{GFP/+}$ WT, reverse (5′-GGAGCGGGAGAAATGGATATG-3′); *Atoh1*$^{GFP/+}$ WT, forward (5′-AGGGTCAGCTTGCCGTAGGT-3′); and *Atoh1*$^{GFP/+}$ mutant, forward (5′-GCGATGATGGCACAGAAGG-3′), *Atoh1*$^{GFP/+}$ mutant, reverse (5′-GAAGGGCATTTGGTTGTCTCAG-3′).

For qPCR, total RNA was isolated with an RNeasy Mini Extraction Kit (QIAGEN), and then cDNA was synthesized using SuperScript VILO cDNA Kit (Invitrogen, Thermo Fisher Scientific). TaqMan Fast Advanced Mix and Assays (Applied Biosystems) were used to perform qPCR reactions on a CFX Connect Real-Time System (Bio-Rad). All qPCR reactions were performed in triplicate, and the relative quantification of gene expression was analyzed using the ΔΔCt method (87). These

results were normalized to an averaged value of 3 housekeeping genes (*B2M*, *Hprt*, and *Rplp0* for *Sox2*$^{CreERT2/+}$ or *GAPDH*, *Hprt*, and *Snrpd3* for *Ctnnb1*$^{fl(ex3)/+}$ experiments) (31). The following probes were used: *Axin2* (Mm00443610_m1); *B2M* (MM00437762_m1); *Ctnnb1* (exon 3) (Mm00483029_g1); *Ctnnb1* (exon 13) Mm00483039_m1; *GAPDH* (Mm9999999915_g1); *Hes1* (Mm01342805_m1), *Hes5* (Mm00439311_g1); *Hey1* (mm00468865_m1); *Hprt* (Mm01545399_m1); *Lef1* (Mm00550265_m1); *Lgr5* (Mm00438905_m1); *Rplp0* (Mm00725448_s1); *Snrpd3* (Mm01151268_m1); and *Sox2* (Mm03053810_s1).

Auditory measurements. Auditory brainstem responses and DPOAEs were measured as previously described (58). Briefly, mice were anesthetized with i.p. injection of 100 mg/kg ketamine and 10 mg/kg xylazine. Auditory responses were recorded from a needle electrode placed inferiorly to the tympanic bulla, referenced to an electrode on the vertex of the head, with a ground electrode placed into the hind limb. Tone pip stimuli were delivered in frequencies ranging from 4 to 46 kHZ (4.0, 5.7, 8.0, 11.3, 16.0, 23.0, 31.9, and 46.1 kHZ) up to a sound pressure level (SPL) of 80 dB, in 10-dB steps. At each frequency and intensity, 260 trials were conducted and averaged. DPOAEs were measured by a probe-tip microphone placed into the auditory canal. The sound stimuli used to elicit the DPOAE were two 1-second sine wave tones of differing frequencies (F2 = 1.22 × F2). F2 ranged from 4 to 46 kHz, and the 2 tones were stepped up from 20 to 80 dB SPL in 10-dB increments. The amplitude of the cubic distortion product was 2 × F1-F2. The threshold was calculated as a DPOAE of greater than 5 dB SPL and 2 SDs above the noise floor for each frequency. For analysis of ABR and DPOAE responses, a lack of a response was designated at the highest sound level, 80 dB SPL.

IHC. Neonatal and adult cochleae were isolated and fix in 4% paraformaldehyde in PBS for 30 to 40 minutes (in PBS, pH7.4; Electron Microscopy Services) for further processing. Adult tissues were decalcified in 120 mM EDTA for 24 to 36 hours at 4°C. Tissues from mice of both ages were dissected into 3 turns, with the Reissner's and tectorial membranes and stria vascularis removed. Tissues were then washed with 0.1% Triton X-100 (in PBS) 3 times for 5 to 10 minutes each and blocked with 5% donkey serum, 0.1% Triton X-100, 1% BSA, and 0.02% sodium azide (NaN_3) in PBS at pH 7.4 for 1 hour at room temperature. Next tissues were incubated with primary antibodies in the same blocking solution overnight at 4°C. The following day, tissues were washed with 0.1% Triton X-100 in PBS and incubated with secondary antibodies diluted in PBS containing 0.1% Triton X-100, 1% BSA, and 0.02% NaN_3 for 2 hours at room temperature. After washing with PBS 3 times for 10 minutes, tissues were mounted in Antifade Fluorescence Mounting Medium (Dako) and coverslipped.

The following antibodies were used: rabbit anti–myosin 7a (1:500 to 1:1,000; Proteus Bioscience; catalog 25-6790); mouse anti–myosin 7a (1:500; Developmental Studies Hybridoma Bank, University of Iowa; catalog 138-1-c); goat anti-Sox2 (1:200 to 1:400; Santa Cruz Biotechnology; catalog SC17320); rabbit anti-Atoh1 (1:1,000; Proteintech; catalog 21215-1AP); guinea pig anti-Gfi1 (1:1,000; gift of H. Bellen, Department of Molecular and Human Genetics, Baylor College of Medicine, Houston, Texas, USA) (32); rabbit anti-Ki67 (1:500; Abcam; catalog ab16667); mouse anti-BrdU (1:500; Thermo Fisher Scientific; catalog B35128); rabbit anti-Lef1 (1:400; Cell Signaling Technology; catalog 2230s); and Alexa Fluor donkey anti-goat 488 (A11055), Alexa Fluor donkey anti-goat 546 (A11056), Alexa Fluor donkey anti-goat 647 (A21447), Alexa Fluor donkey anti-mouse 488 (A21202), Alexa Fluor donkey anti-mouse 546 (A10036), Alexa Fluor donkey anti-mouse 647 (A31571), Alexa Fluor donkey anti-rabbit 488 (A21206, Alexa Fluor donkey anti-rabbit 546 (A10040), Alexa Fluor donkey anti-rabbit 647 (A31573) secondary antibodies (1:250 to 1:500; Life Technologies, Thermo Fisher Scientific). Fluoresecence-conjugated phalloidin (1:1,000; Invitrogen, Thermo Fisher Scientific; catalog A22283); DAPI (1:10,000; Invitrogen, Thermo Fisher Scientific; catalogD1306); and an Alexa Fluor 555 or 647 EdU Detection Kit (Invitrogen, Thermo Fisher Scientific; catalog C10338/C10340). To assess proliferation in cochleae from mice treated with BrdU following secondary antibody incubation, tissues were washed with PBS and repermeabilized, after which tissues were incubated with 2N HCl in 0.05% Triton X-100 for 1 hour at room temperature. The tissues were then washed with PBS and blocked and immunostained with anti-BrdU as outlined above.

Whole mounts were imaged as *Z*-stacks on a Zeiss LSM700 confocal microscope, and images were captured using Zen Software (Carl Zeiss) and analyzed with ImageJ (NIH) and Photoshop CS6 (Adobe Systems).

ISH. Tissues were harvested on ice, fixed in 4% PFA overnight, and then embedded for cryosectioning as described previously (57). Briefly, tissues were sequentially submerged in 10%, 20%, and 30% sucrose prior to tissue embedment and freezing in 100% OCT (Sakura). Tissue sections were hybridized with commercial probes from Advanced Cell Diagnostics according to the manufacturer's instructions for fixed, frozen sections with colorimetric detection (88). Briefly, sections were washed in 1× PBS for 5 minutes and then treated with H_2O_2 for 10 minutes. Next, sections were permeabilized using target retrieval reagent and proteinase before hybridization. The following Advanced Cell Diagnostics probes were used: *Hes5* (catalog 400991), *DapB* (catalog 310043), *Polr2a* (catalog 310451), and *Sox2* (catalog 401041). WT and *Sox2*$^{CreERT2/+}$ cochleae were processed in parallel, with sections collected on the same slide and subjected to mRNA detection under identical conditions.

Cell quantification. For cell counting, confocal images were analyzed using ImageJ. To quantify EdU-labeled cells and ectopic hair cells in neonatal cochleae, *Z*-stack images were taken of the whole cochleae, which were divided into apical, middle, and basal turns of equal length, and cells were counted from stacks using ImageJ. Other cell counts in the neonatal and the adult cochleae were performed on representative *Z*-stack images of individual turns.

Statistics. Data were analyzed using Microsoft Excel and GraphPad Prism Version 7 (GraphPad Software). A 2-tailed Student's *t* test or ANOVA with post hoc testing was used to calculate statistical significance. A *P* value of less than 0.05 was considered statistically significant. Data shown in the figures represent the mean ± SD. For all experiments, *n* values represent the number of animals examined.

Study approval. All experimental protocols were approved by the IACUC of Stanford University.

Author contributions

PJA, YD, and AGC designed the studies. PJA, YD, SG, WL, EHN, and TU conducted the experiments. PJA, YD, and AGC analyzed the data and wrote the manuscript.

Acknowledgments

We are deeply grateful to the members of our laboratory; R. Nusse, S. Heller, and B. Hartman (all from Stanford Univer-

sity, Stanford, CA, USA) for insightful comments and fruitful discussions of the manuscript; J. Eide, K. Han, Q. Wang, T. Jan, and W. Dong (all from Stanford University, Stanford, CA, USA) for excellent technical support; E. Rubel (University of Washington, Seattle, WA, USA) for sharing *Pou4f3-DTR* mice; W. Richardson (University College London, London, United Kingdom) for sharing *Fgfr3-iCre* mice; M. Taketo (Kyoto University, Kyoto, Japan) for sharing *Ctnnb1-flox(ex3)* mice; and H. Bellen (Baylor College of Medicine, Houston, TX, USA) for the providing Gfi1 antibodies. This work was supported by the Lucile Packard Foundation for Children's Health, Stanford; the NIH National Center for Advancing Translational Sciences – Clinical and Translational Science Awards (NCATS-CTSA) program (UL1TR001085); the Child Health Research Institute of Stanford University; a Garnett Passe and Rodney Williams Memorial Foundation Research Training Grant (to PJA); the Science and Technology Research Program of the Liaoning Education Department (LK201647, to YD); the National Institute on Deafness and other Communication Disorders (NIDCD), NIH (F32DC014623, to EHN, and K08DC011043 and RO1DC01910); the Department of Defense (MR130316); the Akiko Yamazaki and Jerry Yang Faculty Scholar Fund; the California Initiative in Regenerative Medicine (RN3-06529, to AGC); and the Yu and Oberndorf families.

Address correspondence to: Alan G. Cheng, 801 Welch Road, Department of Otolaryngology-HNS, Stanford, California 94305, USA. Phone: 650.725.6500; Email: aglcheng@stanford.edu.

1. Avilion AA, Nicolis SK, Pevny LH, Perez L, Vivian N, Lovell-Badge R. Multipotent cell lineages in early mouse development depend on SOX2 function. *Genes Dev*. 2003;17(1):126–140.
2. Masui S, et al. Pluripotency governed by Sox2 via regulation of Oct3/4 expression in mouse embryonic stem cells. *Nat Cell Biol*. 2007;9(6):625–635.
3. Takahashi K, Yamanaka S. Induction of pluripotent stem cells from mouse embryonic and adult fibroblast cultures by defined factors. *Cell*. 2006;126(4):663–676.
4. Yu J, et al. Induced pluripotent stem cell lines derived from human somatic cells. *Science*. 2007;318(5858):1917–1920.
5. Bylund M, Andersson E, Novitch BG, Muhr J. Vertebrate neurogenesis is counteracted by Sox1-3 activity. *Nat Neurosci*. 2003;6(11):1162–1168.
6. Ellis P, et al. SOX2, a persistent marker for multipotential neural stem cells derived from embryonic stem cells, the embryo or the adult. *Dev Neurosci*. 2004;26(2-4):148–165.
7. Favaro R, et al. Hippocampal development and neural stem cell maintenance require Sox2-dependent regulation of Shh. *Nat Neurosci*. 2009;12(10):1248–1256.
8. Graham V, Khudyakov J, Ellis P, Pevny L. SOX2 functions to maintain neural progenitor identity. *Neuron*. 2003;39(5):749–765.
9. Hutton SR, Pevny LH. SOX2 expression levels distinguish between neural progenitor populations of the developing dorsal telencephalon. *Dev Biol*. 2011;352(1):40–47.
10. Taranova OV, et al. SOX2 is a dose-dependent regulator of retinal neural progenitor competence. *Genes Dev*. 2006;20(9):1187–1202.
11. Kiernan AE, et al. Sox2 is required for sensory organ development in the mammalian inner ear. *Nature*. 2005;434(7036):1031–1035.
12. Driskell RR, Giangreco A, Jensen KB, Mulder KW, Watt FM. Sox2-positive dermal papilla cells specify hair follicle type in mammalian epidermis. *Development*. 2009;136(16):2815–2823.
13. Kamachi Y, Uchikawa M, Collignon J, Lovell-Badge R, Kondoh H. Involvement of Sox1, 2 and 3 in the early and subsequent molecular events of lens induction. *Development*. 1998;125(13):2521–2532.
14. Okubo T, Clark C, Hogan BL. Cell lineage mapping of taste bud cells and keratinocytes in the mouse tongue and soft palate. *Stem Cells*. 2009;27(2):442–450.
15. Okubo T, Pevny LH, Hogan BL. Sox2 is required for development of taste bud sensory cells. *Genes Dev*. 2006;20(19):2654–2659.
16. Que J, Luo X, Schwartz RJ, Hogan BL. Multiple roles for Sox2 in the developing and adult mouse trachea. *Development*. 2009;136(11):1899–1907.
17. Que J, et al. Multiple dose-dependent roles for Sox2 in the patterning and differentiation of anterior foregut endoderm. *Development*. 2007;134(13):2521–2531.
18. Fantes J, et al. Mutations in SOX2 cause anophthalmia. *Nat Genet*. 2003;33(4):461–463.
19. Kelberman D, et al. Mutations within Sox2/SOX2 are associated with abnormalities in the hypothalamo-pituitary-gonadal axis in mice and humans. *J Clin Invest*. 2006;116(9):2442–2455.
20. Sisodiya SM, et al. Role of SOX2 mutations in human hippocampal malformations and epilepsy. *Epilepsia*. 2006;47(3):534–542.
21. Arnold K, et al. Sox2(+) adult stem and progenitor cells are important for tissue regeneration and survival of mice. *Cell Stem Cell*. 2011;9(4):317–329.
22. Brazel CY, et al. Sox2 expression defines a heterogeneous population of neurosphere-forming cells in the adult murine brain. *Aging Cell*. 2005;4(4):197–207.
23. Suh H, Consiglio A, Ray J, Sawai T, D'Amour KA, Gage FH. In vivo fate analysis reveals the multipotent and self-renewal capacities of Sox2+ neural stem cells in the adult hippocampus. *Cell Stem Cell*. 2007;1(5):515–528.
24. Amador-Arjona A, et al. SOX2 primes the epigenetic landscape in neural precursors enabling proper gene activation during hippocampal neurogenesis. *Proc Natl Acad Sci U S A*. 2015;112(15):E1936–E1945.
25. Ferri AL, et al. Sox2 deficiency causes neurodegeneration and impaired neurogenesis in the adult mouse brain. *Development*. 2004;131(15):3805–3819.
26. Julian LM, et al. Opposing regulation of Sox2 by cell-cycle effectors E2f3a and E2f3b in neural stem cells. *Cell Stem Cell*. 2013;12(4):440–452.
27. Gaete M, et al. Spinal cord regeneration in Xenopus tadpoles proceeds through activation of Sox2-positive cells. *Neural Dev*. 2012;7:13.
28. Kempfle JS, Turban JL, Edge AS. Sox2 in the differentiation of cochlear progenitor cells. *Sci Rep*. 2016;6:23293.
29. Woods C, Montcouquiol M, Kelley MW. Math1 regulates development of the sensory epithelium in the mammalian cochlea. *Nat Neurosci*. 2004;7(12):1310–1318.
30. Hertzano R, et al. Transcription profiling of inner ears from Pou4f3(ddl/ddl) identifies Gfi1 as a target of the Pou4f3 deafness gene. *Hum Mol Genet*. 2004;13(18):2143–2153.
31. Vahava O, et al. Mutation in transcription factor POU4F3 associated with inherited progressive hearing loss in humans. *Science*. 1998;279(5358):1950–1954.
32. Varfolomeev EE, et al. Targeted disruption of the mouse Caspase 8 gene ablates cell death induction by the TNF receptors, Fas/Apo1, and DR3 and is lethal prenatally. *Immunity*. 1998;9(2):267–276.
33. Hasson T, et al. Unconventional myosins in inner-ear sensory epithelia. *J Cell Biol*. 1997;137(6):1287–1307.
34. Oesterle EC, Campbell S, Taylor RR, Forge A, Hume CR. Sox2 and JAGGED1 expression in normal and drug-damaged adult mouse inner ear. *J Assoc Res Otolaryngol*. 2008;9(1):65–89.
35. Dabdoub A, et al. Sox2 signaling in prosensory domain specification and subsequent hair cell differentiation in the developing cochlea. *Proc Natl Acad Sci U S A*. 2008;105(47):18396–18401.
36. Ahmed M, Wong EY, Sun J, Xu J, Wang F, Xu PX. Eya1-Six1 interaction is sufficient to induce hair cell fate in the cochlea by activating Atoh1 expression in cooperation with Sox2. *Dev Cell*. 2012;22(2):377–390.
37. Ahmed M, Xu J, Xu PX. EYA1 and SIX1 drive the neuronal developmental program in cooperation with the SWI/SNF chromatin-remodeling complex and SOX2 in the mammalian inner ear. *Development*. 2012;139(11):1965–1977.
38. Puligilla C, Kelley MW. Dual role for Sox2 in specification of sensory competence and regulation of Atoh1 function. *Dev Neurobiol*. 2017;77(1):3–13.
39. Pan W, Jin Y, Chen J, Rottier RJ, Steel KP, Kiernan AE. Ectopic expression of activated notch or SOX2 reveals similar and unique roles in the development of the sensory cell progenitors in the mammalian inner ear. *J Neurosci*. 2013;33(41):16146–16157.
40. Neves J, Parada C, Chamizo M, Giráldez F. Jagged 1 regulates the restriction of Sox2 expression in

the developing chicken inner ear: a mechanism for sensory organ specification. *Development*. 2011;138(4):735–744.
41. Neves J, Vachkov I, Giraldez F. Sox2 regulation of hair cell development: incoherence makes sense. *Hear Res*. 2013;297:20–29.
42. Ruben RJ, Van de Water T, Polesky A. Cell kinetics of the 11 and 12-day mouse otocysts. *Laryngoscope*. 1971;81(10):1708–1718.
43. Cox BC, et al. Spontaneous hair cell regeneration in the neonatal mouse cochlea in vivo. *Development*. 2014;141(4):816–829.
44. Tong L, et al. Selective deletion of cochlear hair cells causes rapid age-dependent changes in spiral ganglion and cochlear nucleus neurons. *J Neurosci*. 2015;35(20):7878–7891.
45. Bramhall NF, Shi F, Arnold K, Hochedlinger K, Edge AS. Lgr5-positive supporting cells generate new hair cells in the postnatal cochlea. *Stem Cell Reports*. 2014;2(3):311–322.
46. Lin V, Golub JS, Nguyen TB, Hume CR, Oesterle EC, Stone JS. Inhibition of Notch activity promotes nonmitotic regeneration of hair cells in the adult mouse utricles. *J Neurosci*. 2011;31(43):15329–15339.
47. Wang GP, et al. Notch signaling and Atoh1 expression during hair cell regeneration in the mouse utricle. *Hear Res*. 2010;267(1-2):61–70.
48. Chen P, Johnson JE, Zoghbi HY, Segil N. The role of Math1 in inner ear development: Uncoupling the establishment of the sensory primordium from hair cell fate determination. *Development*. 2002;129(10):2495–2505.
49. Hume CR, Bratt DL, Oesterle EC. Expression of LHX3 and SOX2 during mouse inner ear development. *Gene Expr Patterns*. 2007;7(7):798–807.
50. Rose MF, et al. Math1 is essential for the development of hindbrain neurons critical for perinatal breathing. *Neuron*. 2009;64(3):341–354.
51. Cox BC, et al. Spontaneous hair cell regeneration in the neonatal mouse cochlea in vivo. *Development*. 2014;141(4):816–829.
52. Stamos JL, Weis WI. The β-catenin destruction complex. *Cold Spring Harb Perspect Biol*. 2013;5(1):a007898.
53. Harada N, et al. Intestinal polyposis in mice with a dominant stable mutation of the beta-catenin gene. *EMBO J*. 1999;18(21):5931–5942.
54. Chai R, et al. Wnt signaling induces proliferation of sensory precursors in the postnatal mouse cochlea. *Proc Natl Acad Sci U S A*. 2012;109(21):8167–8172.
55. Shi F, Hu L, Edge AS. Generation of hair cells in neonatal mice by β-catenin overexpression in Lgr5-positive cochlear progenitors. *Proc Natl Acad Sci U S A*. 2013;110(34):13851–13856.
56. Behrens J, et al. Functional interaction of beta-catenin with the transcription factor LEF-1. *Nature*. 1996;382(6592):638–642.
57. Jan TA, et al. Tympanic border cells are Wnt-responsive and can act as progenitors for postnatal mouse cochlear cells. *Development*. 2013;140(6):1196–1206.
58. Huth ME, et al. Designer aminoglycosides prevent cochlear hair cell loss and hearing loss. *J Clin Invest*. 2015;125(2):583–592.
59. Cafaro J, Lee GS, Stone JS. Atoh1 expression defines activated progenitors and differentiating hair cells during avian hair cell regeneration. *Dev Dyn*. 2007;236(1):156–170.
60. Liu Z, et al. Regulation of p27Kip1 by Sox2 maintains quiescence of inner pillar cells in the murine auditory sensory epithelium. *J Neurosci*. 2012;32(31):10530–10540.
61. Millimaki BB, Sweet EM, Riley BB. Sox2 is required for maintenance and regeneration, but not initial development, of hair cells in the zebrafish inner ear. *Dev Biol*. 2010;338(2):262–269.
62. Nakamura Y, de Paiva Alves E, Veenstra GJ, Hoppler S. Tissue- and stage-specific Wnt target gene expression is controlled subsequent to β-catenin recruitment to cis-regulatory modules. *Development*. 2016;143(11):1914–1925.
63. Buchert M, et al. Genetic dissection of differential signaling threshold requirements for the Wnt/beta-catenin pathway in vivo. *PLoS Genet*. 2010;6(1):e1000816.
64. Kormish JD, Sinner D, Zorn AM. Interactions between SOX factors and Wnt/beta-catenin signaling in development and disease. *Dev Dyn*. 2010;239(1):56–68.
65. Sarkar A, et al. Sox2 Suppresses Gastric Tumorigenesis in Mice. *Cell Rep*. 2016;16(7):1929–1941.
66. Otsubo T, Akiyama Y, Yanagihara K, Yuasa Y. SOX2 is frequently downregulated in gastric cancers and inhibits cell growth through cell-cycle arrest and apoptosis. *Br J Cancer*. 2008;98(4):824–831.
67. Chen Y, et al. The molecular mechanism governing the oncogenic potential of SOX2 in breast cancer. *J Biol Chem*. 2008;283(26):17969–17978.
68. Ni W, et al. Extensive supporting cell proliferation and mitotic hair cell generation by in vivo genetic reprogramming in the neonatal mouse cochlea. *J Neurosci*. 2016;36(33):8734–8745.
69. Abdolazimi Y, Stojanova Z, Segil N. Selection of cell fate in the organ of Corti involves the integration of Hes/Hey signaling at the Atoh1 promoter. *Development*. 2016;143(5):841–850.
70. Zine A, et al. Hes1 and Hes5 activities are required for the normal development of the hair cells in the mammalian inner ear. *J Neurosci*. 2001;21(13):4712–4720.
71. Doetzlhofer A, Basch ML, Ohyama T, Gessler M, Groves AK, Segil N. Hey2 regulation by FGF provides a Notch-independent mechanism for maintaining pillar cell fate in the organ of Corti. *Dev Cell*. 2009;16(1):58–69.
72. Maass JC, et al. Transcriptomic Analysis of Mouse Cochlear Supporting Cell Maturation Reveals Large-Scale Changes in Notch Responsiveness Prior to the Onset of Hearing. *PLoS ONE*. 2016;11(12):e0167286.
73. Yamamoto N, Tanigaki K, Tsuji M, Yabe D, Ito J, Honjo T. Inhibition of Notch/RBP-J signaling induces hair cell formation in neonate mouse cochleas. *J Mol Med*. 2006;84(1):37–45.
74. Korrapati S, Roux I, Glowatzki E, Doetzlhofer A. Notch signaling limits supporting cell plasticity in the hair cell-damaged early postnatal murine cochlea. *PLoS ONE*. 2013;8(8):e73276.
75. Hartman BH, Basak O, Nelson BR, Taylor V, Bermingham-McDonogh O, Reh TA. Hes5 expression in the postnatal and adult mouse inner ear and the drug-damaged cochlea. *J Assoc Res Otolaryngol*. 2009;10(3):321–340.
76. Lanford PJ, Shailam R, Norton CR, Gridley T, Kelley MW. Expression of Math1 and HES5 in the cochleae of wildtype and Jag2 mutant mice. *J Assoc Res Otolaryngol*. 2000;1(2):161–171.
77. Maass JC, et al. Changes in the regulation of the Notch signaling pathway are temporally correlated with regenerative failure in the mouse cochlea. *Front Cell Neurosci*. 2015;9:110.
78. Doetzlhofer A, Avraham KB. Insights into inner ear-specific gene regulation: Epigenetics and non-coding RNAs in inner ear development and regeneration. *Semin Cell Dev Biol*. 2017;65:69–79.
79. Cox BC, Liu Z, Lagarde MM, Zuo J. Conditional gene expression in the mouse inner ear using Cre-loxP. *J Assoc Res Otolaryngol*. 2012;13(3):295–322.
80. Eagleson KL, et al. Disruption of Foxg1 expression by knock-in of cre recombinase: effects on the development of the mouse telencephalon. *Neuroscience*. 2007;148(2):385–399.
81. Shen L, Nam HS, Song P, Moore H, Anderson SA. FoxG1 haploinsufficiency results in impaired neurogenesis in the postnatal hippocampus and contextual memory deficits. *Hippocampus*. 2006;16(10):875–890.
82. Siegenthaler JA, Tremper-Wells BA, Miller MW. Foxg1 haploinsufficiency reduces the population of cortical intermediate progenitor cells: effect of increased p21 expression. *Cereb Cortex*. 2008;18(8):1865–1875.
83. Li W, et al. Notch inhibition induces mitotically generated hair cells in mammalian cochleae via activating the Wnt pathway. *Proc Natl Acad Sci U S A*. 2015;112(1):166–171.
84. Avraham KB. Hear come more genes! *Nat Med*. 1998;4(11):1238–1239.
85. Young KM, Mitsumori T, Pringle N, Grist M, Kessaris N, Richardson WD. An Fgfr3-iCreER(T2) transgenic mouse line for studies of neural stem cells and astrocytes. *Glia*. 2010;58(8):943–953.
86. Madisen L, et al. A robust and high-throughput Cre reporting and characterization system for the whole mouse brain. *Nat Neurosci*. 2010;13(1):133–140.
87. Livak KJ, Schmittgen TD. Analysis of relative gene expression data using real-time quantitative PCR and the 2(-Delta Delta C(T)) Method. *Methods*. 2001;25(4):402–408.
88. Wang F, et al. RNAscope: a novel in situ RNA analysis platform for formalin-fixed, paraffin-embedded tissues. *J Mol Diagn*. 2012;14(1):22–29.